https://doi.org/10.5194/egusphere-2026-881
Preprint. Discussion started: 5 March 2026

Integrating reservoirs and lakes in the CoSWAT global hydrological model

Jose P. Teran[1], Celray J. Chawanda[1,2], Albert Nkwasa[1,3], Inne Vanderkelen[4,5], Jeffrey G. Arnold[6], Ann Van Griensven[1,7]

[1] Department of Water and Climate, Vrije Universiteit Brussel, Brussel, Elsene 1050, Belgium
[2] Blackland Research & Extension Center, Texas A&M Agrilife Research, Temple, 76502 TX, USA
[3] Water Security Research Group, Biodiversity and Natural Resources Program, International Institute for Applied Systems Analysis (IIASA), A-2361 Laxenburg, Austria
[4] Department of Earth and Environmental Sciences, KU Leuven, Leuven 3000, Belgium
[5] Royal Meteorological Institute of Belgium (RMIB), Brussels, Uccle 1180, Belgium
[6] Grassland Soil and Water Research Laboratory, USDA Agricultural Research Service (ARS), Temple, 76502 TX, USA
[7] Institute for Water Education (IHE) Delft, 2611 AX Delft, Netherlands

Correspondence to: Jose P. Teran (jose.pablo.teran.orsini@vub.be)

Abstract. Global water models are essential tools for assessing water resource challenges in the context of climate change, land use changes, and human activities. The CoSWAT Global Water model is a global application of the Soil and Water Assessment Tool (SWAT +). It is a high-resolution tool designed to simulate water systems using a basin-oriented structure. The CoSWAT model currently lacks a realistic representation of reservoirs and lakes, limiting its ability to adequately represent basins where these water bodies play a significant hydrological role. The scarcity and limited accessibility of global reservoir operation or lake outflow data make it challenging to represent these water bodies with the current tools that SWAT+ supports, particularly at a global scale. In this study, we address this limitation by combining commonly used reservoir and lake modelling schemes from other global water models and the capabilities of SWAT+. Moreover, to model irrigation reservoirs, we implemented an approach that combines global datasets with a topological method to estimate irrigation demand for each reservoir. With these new implementations, the CoSWAT model was restructured for selected regions worldwide, where validation of reservoir or lake storage, inflow, and outflow was performed, and the impact of these implementations on streamflow performance was assessed. The results show that the model captures storage dynamics with reasonable performance, comparable to other state-of-the-art global models, and demonstrate a general improvement (70% of evaluated stations) in streamflow representation following the integration of these water bodies. The new methodological advancements represent a substantial improvement for the CoSWAT global model, enabling more robust and realistic assessments of inland water systems at the global scale.

1 Introduction

Rivers and lakes are essential for supporting ecosystems, providing access to water resources, preserving biodiversity, and regulating the water cycle. At the same time, reservoirs are crucial for water supply to different sectors, energy generation, and

https://doi.org/10.5194/egusphere-2026-881
Preprint. Discussion started: 5 March 2026

flood control. The combination of anthropogenic climate change, driven by alterations in the land use and land cover (LULC), human activities, and socio-economic shifts, has unequivocally affected climate conditions and the functioning of water resources worldwide (Calvin et al., 2023). Global studies based on historical observational records and Global Water Models (GWMs) have found that drying and wetting trends in river flows can be attributed to anthropogenic climate change (Gudmundsson et al., 2021). In addition, global change-induced modifications are transgressing planetary boundaries for freshwater change and ecological functioning of river ecosystems (Porkka et al., 2024; Thompson et al., 2021), and changing erosion and sediment dynamics (Nkwasa et al., 2022). These processes affect reservoirs globally, impacting water security with respect to the production of drinking water and use of water resources across sectors, such as energy and agriculture (Perera et al., 2022; Wisser et al., 2013). Multiple studies indicate that the influence of climate change on lake water levels is unmistakable. Drying and wetting trends are intensifying (Bai et al., 2024), as is ecosystem degradation(Grant et al., 2021; La Fuente et al., 2024; Woolway and Merchant, 2019).

In the context of significant changes in the world's inland waters resulting from global changes, GWMs are designed to simulate hydrological processes at the planetary scale and serve as a key tool for informing policymakers and stakeholders across sectors and governance levels in developing adaptation and mitigation plans. Various types exist, among them, Global Hydrological Models (GHMs), Land Surface Models (LSMs), and Dynamic Global Vegetation Models (DGVMs). Almost all models integrate multiple components of water storage; however, not all models consider reservoirs, and even fewer account for lakes (Telteu et al., 2021). Since most GWMs have a gridded structure, generally at 0.5° x 0.5° resolution, lakes and reservoirs, if accounted for, are considered as representative water bodies in the model grid, not as individual, explicit water bodies, requiring scaling procedures to analyze them further individually (Ayala et al., 2026). Moreover, most studies in the Global Lake Sector of the Inter-sectoral Impact Model Intercomparison Project (ISIMIP) have not yet accounted for water balance, lake inputs and withdrawals, or lake stage variability, and simulate only heat exchange (Golub et al., 2022), disregarding advective fluxes, which can be a significant omission in systems with large storage fluctuations (Fenocchi et al., 2017). Omitting key processes related to the hydrology and consequently of the biogeochemistry of lakes undermines the research oriented towards these ecosystems, as this information is invaluable for their management, which underscores the importance of providing the lake scientific community with models and frameworks that can deliver insights into the water budget of lakes (Ayala et al., 2026; Janssen et al., 2019).

Several schemes and frameworks for representing lakes and reservoirs have been developed and applied in hydrological models. Many methods estimate outflow from water bodies using simple relationships among storage, residence time, or other properties, typically parameterized with polynomial or exponential coefficients (Coe, 2000; Döll et al., 2003; Meigh et al., 1999; Terink et al., 2015). Many others, generally but not exclusively oriented towards flood control reservoirs, utilize sets of rules to determine outflow based on storage and/or outflow thresholds (Burek et al., 2020; Yassin et al., 2019), or target water level, and their timing during the year (Dang et al., 2020). Specific models use naturalized simulations (i.e., simulations without reservoirs in the model's network) of streamflow at the reservoir outflow location to derive the reservoir's release (Haddeland

https://doi.org/10.5194/egusphere-2026-881
Preprint. Discussion started: 5 March 2026

et al., 2006). Primarily based on the H06 scheme (Hanasaki et al., 2006), many global or large scale models utilize a retrospective approach by which past inflows in the simulation define a release target, and in combination with the properties of the reservoir, define an actual release, such as the H08 model (Hanasaki et al., 2018), the LPJmL model (Biemans et al., 2011), the LHF and CamaFlood models (Shin et al., 2019, 2020), and the mizuRoute routing scheme (Gharari et al., 2024; Vanderkelen et al., 2022). Similarly, the Water Balance Model (Grogan et al., 2022; Wisser et al., 2010) and PCR-GLOBWB (Sutanudjaja et al., 2018; Van Beek et al., 2011) use historical inflows to derive releases.

The Soil and Water Assessment Tool (SWAT+) is a semi-distributed, process-based, watershed model capable of simulating several hydrological processes, plant growth, erosion, sediment, and pollutant transport, among others (Arnold et al., 1998, 2012; Bieger et al., 2017). The model's smallest element is the Hydrological Response Unit (HRU), an area with a unique combination of slope class, soil type, and land use classification, which is aggregated into Landscape Units (LSUs), sub-basins, and ultimately to a watershed. The water and mass balance is central in the model, and is used in the calculation of hydrological processes in the land phase at HRUs and further aggregated into LSUs, while routing processes of water and constituents occur in the river reaches of the hydrographic network, which is connected to the model structure (Neitsch et al., 2011). The SWAT+ model can account for lakes and reservoirs as another type of object in the model structure, typically called "water areas", which become part of the river network, and are connected to HRUs and LSUs (Bieger et al., 2017). The outflow, or release, in reservoirs and lakes, is typically established by the use of decision tables, a flexible and robust framework by which a set of conditions and actions can be specified (Arnold et al., 2018), therefore, a rule-based approach can be established to simulate these water bodies.

The SWAT+ model has been widely applied at local (Tan et al., 2020), regional, and continental scales (Abbaspour et al., 2015; Chawanda, Arnold, et al., 2020; Chawanda et al., 2024; Nkwasa et al., 2022; Nkwasa et al., 2024). Most recently, it has been applied on a global scale, resulting in the Community SWAT+ (CoSWAT) v1 GHM (Chawanda et al., 2025). The CoSWAT v1 model is a high-resolution GHM (spatial input data at 0.2° resolution) that, unlike most GHMs, follows the SWAT+ semi-distributed structure rather than a gridded one, thereby enabling more explicit representation of land and water components while balancing the level of detail and computational demand. The structure of the CoSWAT v1 GHM was developed using the CoSWAT Framework, a tool that enables automatic generation of the model's components, based on Chawanda et al. (2020), with methodological advancements to enhance global applicability and reproducibility. Despite its promising results and reasonable performance, the CoSWAT v1 GHM presents limitations and spaces for improvement. It has been proven that the implementation of reservoirs, lakes, and management practices significantly affects the performance of hydrological models (Chawanda et al., 2020; Zajac et al., 2017). However, the model does not include lakes or reservoirs as components in its structure, which may be a significant omission in many regions where such water bodies play an important role in hydrological processes. This, combined with a lack of representation of water management (e.g., agricultural practices), is potentially the cause of bad model performance for streamflow in many locations (Chawanda et al., 2025).

https://doi.org/10.5194/egusphere-2026-881
Preprint. Discussion started: 5 March 2026

The exclusion of lakes and reservoirs from the model structure was mainly driven by the difficulty of explicitly resolving water bodies within the river network using the tools available in the CoSWAT Framework. An additional limitation of the CoSWAT v1 GHM stems from the rule-based approach that SWAT+ uses to simulate reservoir outflows. Although large scale studies have demonstrated that reservoir operation decision tables can be derived and applied successfully (Chawanda et al., 2020a; Wu et al., 2020) these approaches rely heavily on reference data. As a result, transferring such methods at a global scale remains challenging with current SWAT+ capabilities due to substantial data requirements.

Here, we establish methodological advances to address those limitations in representing water bodies and water management by:

- developing a robust and flexible algorithm in the CoSWAT Framework to resolve water areas into the model structure and river network,
- developing a reservoir and lake outflow calculation approach with global applicability, combining the strengths of what SWAT+ supports and state-of-the-art schemes used in other GWMs,
- and introducing an automatic approach in the CoSWAT Framework to define irrigation application and demand to irrigation purpose reservoirs.

The new implementations were applied in selected regions worldwide with sufficient data availability, where the model's ability to represent reservoir or lake storage, inflows, and outflows was tested. The model's streamflow performance with and without the new implementations was also compared to assess their impacts. The study establishes a baseline for a new and improved version of the CoSWAT GHM and the CoSWAT Framework that better represents global inland waters, provides insights into the capabilities of generalized, parametric schemes for simulating lakes and reservoirs in GWMs, and outlines future directions for improvement.

2 Methodology

2.1 Global Datasets

A summary of the datasets used in this study is provided in Table 1. This includes data on the setup of CoSWAT, the reservoir/lake simulation schemes, irrigation demand, and model evaluation. Datasets for model setup provide mappings of the physical properties of land, soil, and climate forcings. The topography was defined using the Global Aster Digital Elevation Model (Abrams, 2016). The reference land cover map was obtained from the ESA CCI Land Cover Product (ESA, 2017), while soil classification and properties were derived from the FAO Harmonized World Soil Database (Fischer et al., 2008). The CoSWAT model requires daily precipitation, maximum and minimum temperatures, solar radiation, wind speed, and relative humidity as weather inputs, all of which are available in the GWSP3-W5E5 dataset (Lange et al., 2022).

Some datasets were used both in the setup and in the configuration of the reservoir/lake simulation scheme. This includes the HydroLakes and GranD datasets, which were used to integrate lakes and reservoirs into the model's structure based on their

https://doi.org/10.5194/egusphere-2026-881
Preprint. Discussion started: 5 March 2026

geographic locations. The physical and operational properties, together with the depth-area-volume (h-A-V) relationships from the GLOBathy dataset, were used to establish the new reservoir/lake simulation scheme. Moreover, the FAO Irrigation Area dataset provided key inputs to identify irrigated HRUs, which were subsequently configured to represent irrigation application and demand. For model evaluation, data from the Global Runoff Data Centre (GRDC; https://grdc.bafg.de/data/data_portal) were used to evaluate streamflow, and a combination of three data sources, GRS (Li, 2023), ResOpsUs (Steyaert et al., 2022) and (Yassin, 2018), was used to evaluate the model's storage, inflow, and outflow outputs under the new implementations.

Table 1: Datasets used in this study, resolution, purpose of use, and source

Dataset	Description	Resolution	Use	Source
ASTER GDEM	Global Digital Elevation Model (DEM)	0.01° (Resampled)	Model Setup	Abrams (2016)
ESA CCI Land Cover	LULC Map of 2015	0.01° (Resampled)		ESA (2017)
FAO HWSD	Soil classes and properties	0.01° (Resampled)		Fischer et al. (2008)
GSWP3-W5E5	Reanalysis climate dataset	0.05°		Lange et al. (2022)
HydroLakes	Global lake map and properties	Vector Based	Model Setup and reservoir/lake simulation scheme	Messager et al. (2016)
GranD	Global reservoir/dam map and properties	Vector Based		Lehner et al. (2011)
GLOBathy	Global lake/reservoir bathymetric relationships	-		Khazaei et al. (2022)
FAO Irrigation Area	Global map of the amount of area equipped for irrigation	0.083°	Irrigation application and demand	Siebert et al. (2013)
GRDC	Observed streamflow data	Daily and monthly	Model evaluation	Global Runoff Data Centre Data Portal
GRS	Global reservoir storage time series	Monthly		Li (2023)
ResOpsUs	Reservoir storage, inflow, and outflow time series in the United States	Monthly		Steyaert et al. (2022)
Local Reservoir Data	Reservoir storage, inflow, and outflow time series in selected reservoirs	Monthly		Yassin (2018)

2.2 Regions of application

The CoSWAT model is divided into 90 regions (Chawanda et al., 2025) representing one or more large river basins, and each region can be treated as an independent sub-model that can be configured individually. In that sense, 9 regions of the model

https://doi.org/10.5194/egusphere-2026-881
Preprint. Discussion started: 5 March 2026

encompassing several river basins around the world (Figure 1), were selected to apply and evaluate the implementations developed in this study, spanning diverse environmental and operational conditions across nearly all continents, where sufficient data were available for robust evaluation.

The selected regions span several climatic zones worldwide, including tropical, arid, temperate, cold, and polar (frost), according to the Köppen-Geiger classification system (Beck et al., 2023). On the African continent, modelled regions include the Nile River Basin and smaller adjacent subbasins that drain to the Red Sea and the Mediterranean Sea, as well as the Orange River Basin and the coastal regions in the south of the continent. In South America, the simulated area encompasses the Titicaca Basin, the Parana River Basin, the La Plata River Basin, sections of the central Pacific coast basins, and the east Atlantic coast basins. In North America, three regions were included. These include several basins such as the Mississippi River System, the Grande (or Bravo) and Yaqui River Basins, and sections of the Pacific Ocean Seaboard, as well as the Colorado, Sacramento, and Klamath River Basins, and north-western sections of the Pacific Ocean Seaboard. In Asia, the region primarily encompasses the Mekong River Basin and the smaller Chao Phraya and Saigon Basins. In Europe, two regions were set up to represent the central and western sections of the continent, which encompass several River Basins in Italy, France, Germany, Belgium, and the Netherlands, including the Po, Rhine, Meuse, Schelde, Seine, Loire, Garonne, and Rhone, while also covering Spain and Portugal, accounting for the Ebro, Douro, Mino, Lima, Tagus, Guadiana, and Guadalquivir River Basins.

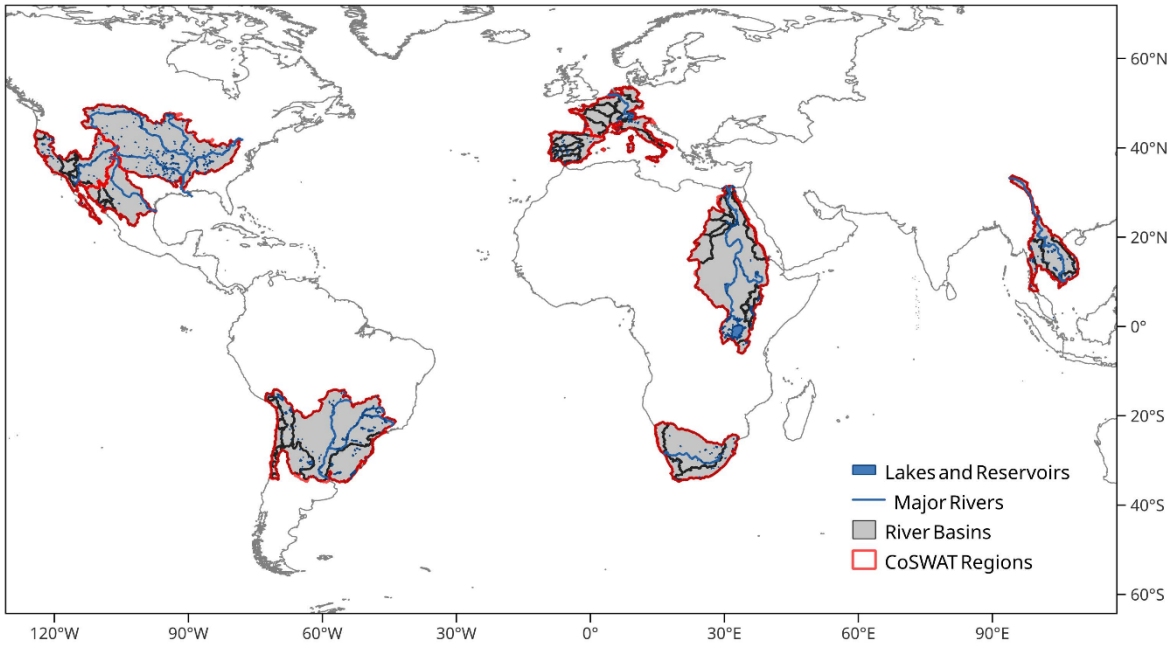

Figure 1: CoSWAT Model regions and River Basins of application for this study. Basin sub-division was done using the HydroBasins dataset (Lehner and Grill, 2013).

https://doi.org/10.5194/egusphere-2026-881
Preprint. Discussion started: 5 March 2026

2.3 Reservoir/Lake integration into model network

In SWAT+, model components are fully vectorized, and lakes or reservoirs are commonly integrated by intersecting their polygon geometries with the river network and spatial model units using GIS tools such as QSWAT+. In this approach, inlets and outlets are identified using geometric rules (e.g., by determining the reach endpoint location relative to the water body), HRUs are converted to water areas, and the model structure is adjusted accordingly. However, this procedure relies primarily on geometric criteria and does not explicitly account for river network topology, which can lead to ambiguous inlet/outlet classification and the exclusion of water bodies, particularly for complex geometries and coarse resolution river networks in global applications. To overcome these limitations, we developed a new lake/reservoir resolution procedure within the CoSWAT Framework (Figure 2), which extends and modifies the original QSWAT+ workflow during model setup by adding an explicit lake/reservoir resolution step, and by adjusting model files to incorporate spatial and physical properties derived from global datasets.

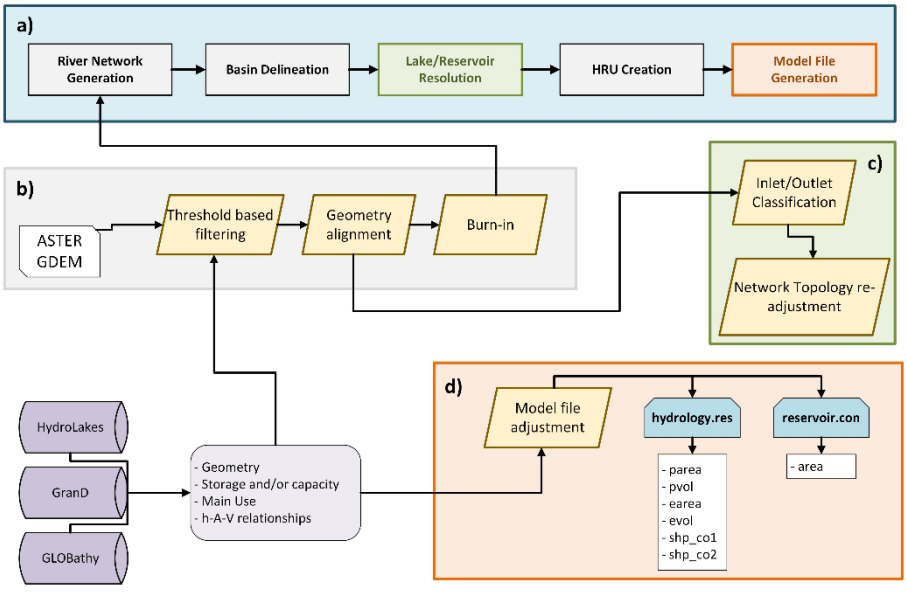

Figure 2: Main steps in model structure generation in a) the CoSWAT-Framework model structure generation, b) pre-processing steps, c) lake and reservoir resolution and integration into the model structure, and c) the adjustment of model files and variables after integration.

The procedure consists of a pre-processing (Figure 2b) with three main steps: (i) threshold-based filtering of water bodies, (ii) alignment of channel-lake intersections to the DEM grid, (iii) burn-in of lake/reservoir elevations into the DEM. With the adjusted DEM, the river network is generated using the Terrain Analysis Using Digital Elevation Models (TauDEM; Tarboton et al., 2009) tool, and the model's sub-basins are delineated. With that information, the resolution of water bodies into the network (Figure 2c) proceeds, and it consists of two steps: (i) enhanced logical identification of inlets and outlets and (ii) re-adjustment of network topological connections. For this study, water bodies smaller than 20 km² were excluded, except when the degree of regulation (i.e., ratio of storage capacity and mean annual outflow) provided by the GranD dataset exceeds 70%,

https://doi.org/10.5194/egusphere-2026-881
Preprint. Discussion started: 5 March 2026

and the area exceeds 10 km². Geometry alignment and DEM burn-in ensure consistent integration of lakes and reservoirs into the river network and prevent the creation of river segments and HRUs smaller than the DEM grid cell, which is required for numerical stability in SWAT+. After the inlets and outlets have been adequately classified and the river network connections have been re-adjusted, the next step is to create the model's HRUs, which proceeds without major adjustments.

After the basic model structure creation is finalized, the framework generates the SWAT+ model files and populates reservoir-related variables (Figure 2d) that cannot be inferred solely from vector geometry (Table 2), therefore relying on information from global datasets. Each water body is classified as natural or regulated based on the HydroLakes dataset attribute "Lake type". For unregulated lakes, properties related to storage are derived from data reported in HydroLakes. For regulated water bodies, this is taken from the GranD dataset. The GLOBathy dataset provides the exponential bathymetric coefficients for the depth-area-volume (h-A-V) relationships of each water body, enabling the determination of surface area from storage or depth. Finally, the GranD's attribute "Main Use" is stored in the model vector files for use in subsequent simulations (e.g., flood control, irrigation, hydropower, water supply).

Table 2: Main hydrological reservoir variables in SWAT+

SWAT+ Variable	Meaning	Model file	Reference data
pvol	*Principal Volume*: Volume needed to fill the reservoir to the principal spillway (m^3).	hydrology.res	HydroLakes or GranD
evol	*Emergency Volume*: Volume needed to fill the reservoir to the emergency spillway (m^3).		
parea	*Principal Area*: Area of the water surface corresponding to the Principal Volume (m^2).		GLOBathy
earea	*Emergency Area*: Area of the water surface corresponding to the Emergency Volume (m^2).		
shp_co1 / shp_co2	*Shape Coefficient 1 / 2:* Shape coefficient to update surface area based on storage.		
area	Area of the water surface (m^2)	reservoir.con	HydroLakes or GranD and GLOBathy

2.4 New lake and reservoir simulation scheme

2.4.1 Water balance

The water balance for lakes and reservoirs in SWAT+ is as follows (Neitsch et al., 2011):

$$\frac{\Delta S}{\Delta t} = P + Q_{in} - E - G - Q_{out} \quad (1)$$

https://doi.org/10.5194/egusphere-2026-881
Preprint. Discussion started: 5 March 2026

where $\frac{\Delta S}{\Delta t}$ (m^3 day^{-1}) is the change in storage per daily times-step of the simulation, P (m^3 day^{-1}) is the precipitation on the surface of the reservoir, Q_{in} (m^3 day^{-1}) is the surface water inflow, E (m^3 day^{-1}) is the evaporation from the water surface, G (m^3 day^{-1}) is the seepage to or from groundwater, and Q_{out} (m^3 day^{-1}) is the release from a regulated reservoir or the outflow from an unregulated lake. Precipitation is a direct input from weather forcings, whereas surface water inflow results from routing water through inlets that drain into the water bodies and from runoff of adjacent HRUs. However, evaporation, groundwater fluxes, and release or outflow need to be calculated during the simulation. Our approach maintains the existing methods to derive evaporation and seepage (Neitsch et al., 2011), as described in detail in Appendix A. By default, SWAT+ simulates outflow or release using decision tables. We enhanced SWAT+ revision 61.0.2 by modifying reservoir-related subroutines and integrating decision tables with two parametric methods to improve global applicability, thereby supporting the CoSWAT GHM. For this, however, we need to distinguish among regulated and unregulated water bodies.

2.4.2 Unregulated lake outflow

To determine unregulated lake outflows, we divide the lake's storage into active and inactive. The threshold for separating active from inactive storage is set to the lake volume corresponding to a depth of 5 meters, following (Döll et al., 2003) for global applications, and is then expressed as a percentage of the principal volume. This is intended to maintain a minimum storage level in the lake at all times, thereby avoiding unrealistic drops; nonetheless, this is a rather arbitrary definition and may require fine-tuning for future applications, particularly in large lakes. The volume corresponding to that depth is determined using the GLOBathy h-A-V relationships. Based on this, the decision table is constructed, and the outflow is determined by the conditions. When the lake storage is above the active volume threshold, the outflow is based on the parametric, time-invariant method developed by Döll et al. (2003):

$$Q_{out} = K_r \cdot (S - s_o \cdot pvol) \cdot \left(\frac{S}{pvol}\right)^{\alpha} \quad (2)$$

where K_r is a release coefficient, in this case fixed to 0.01 day^{-1}, S (m^3) is the current storage in the simulation, s_o the active/inactive storage threshold coefficient, $pvol$ (m^3) is the established principal volume, in this case, derived from Hydrolakes, and α is an exponential coefficient set to 1.5. On the other hand, if the storage is below the inactive/active volume threshold, the outflow is simply zero.

2.4.3 Regulated lake and reservoir release

The release simulation scheme for regulated water bodies is a decision table with multiple release approaches. Central to the approach is a parametric, time-variant, retrospective method, based on the H06 reservoir scheme (Hanasaki et al., 2006) and different implementation approaches (Gharari et al., 2024; Vanderkelen et al., 2022). The H06 scheme distinguishes between irrigation and non-irrigation reservoirs, and its formulation differs accordingly. The key to its approach is that it defines a

https://doi.org/10.5194/egusphere-2026-881
Preprint. Discussion started: 5 March 2026

230 release target and, consequently, an actual release based on past inflows and/or irrigation demands, combined with reservoir properties. A detailed description of the method and its implementation in the CoSWAT model is provided in Appendix A.

As shown in Table 3, the decision table for a regulated water body comprises five conditions at each daily time step. First, the Υ coefficient serves as a threshold that prevents release when reservoir storage falls below this value, thereby ensuring availability during dry months. For this application, Υ was set to 0.15. The second condition applies only during the 235 simulation's warm-up period, during which all water bodies are modeled as natural lakes. This is done to generate historical inflow and irrigation demand data that will subsequently feed the used scheme. For the remainder of the simulation, under the third and fourth conditions, in which reservoir storage is maintained below emergency levels, the downstream release of regulated water bodies is estimated using the parametric H06 scheme. However, as the storage approaches the emergency level (>95%), the release is increased to delay the accumulation of storage. Under the fifth condition, if reservoir storage exceeds 240 5% of the Emergency Volume, the entire volume above that threshold is released.

Table 3: Decision table structure for regulated reservoirs. S: Storage, pvol: Principal volume, evol: Emergency volume, Υ: Reservoir minimum storage coefficient.

Nr.	Condition	Action	Details
1	$S < \gamma \cdot pvol$	No release	-
2	$S > \gamma \cdot pvol$ $S > s_o \cdot pvol$ $Simulation\ year < Warm\ up\ period$	Natural release	Following Eq. (2).
3	$Simulation\ year > Warm\ up\ period$ $S > \gamma \cdot pvol$ $S < evol$	Regulated release 1	Parametric approach based on the H06 scheme.
4	$Simulation\ year > Warm\ up\ period$ $S > 0.95 \cdot evol$	Regulated release 2	Regulated release 1 and total inflow.
5	$Simulation\ year > Warm\ up\ period$ $S > 1.05 \cdot evol$	Emergency release	Release volume of water exceeding the Emergency Volume threshold.

2.5 Irrigation application and demand

The introduction of irrigation application and demand is highly relevant for more accurately representing water management 245 practices in the model. It is also required to fully implement the reservoir/lake simulation scheme for irrigation reservoirs, which require information on downstream irrigation demand to determine their releases. This process was divided into three steps: (i) the definition of irrigated HRUs, (ii) the definition of the source of irrigation water via an irrigation topological connection between model elements, and (iii) the generation of land use management decision tables and the modification of

https://doi.org/10.5194/egusphere-2026-881
Preprint. Discussion started: 5 March 2026

relevant model files. This procedure was also integrated into the CoSWAT Framework to automatically define irrigation for the modelled regions.

The FAO area equipped for irrigation maps is divided into surface-water and groundwater sources. These maps were overlaid with HRUs classified by agricultural land use, and HRUs with an irrigation area fraction exceeding a specified threshold were designated as irrigated. For the regions applied in this study, the threshold was set to 40%. After irrigated HRUs were identified, the irrigation water source was defined (Figure 3). First, whether HRUs used surface or groundwater was based solely on the FAO area equipped for irrigation maps. If an HRU overlaid areas with both sources, the dominant percentage of the equipped area was used as the primary source. To further establish surface water demands for irrigation-purpose reservoirs, a topological connection process was performed following Vanderkelen et al. (2022). This process was used to identify HRUs that require water from an irrigation reservoir. The approach considers the river network downstream of the reservoir outlet for up to 1000 km, encompassing the main river and its tributaries up to second-order. An irrigated HRU with surface water as the primary source, that is hydrologically connected to that portion of the river network, and whose mean elevation is below the mean elevation of the corresponding reservoir, is considered to demand irrigation water from the reservoir. If an HRU demands irrigation water from two or more reservoirs, the demand is weighted to each reservoir based on the ratio of that reservoir's maximum storage capacity to the sum of the maximum storage capacities of all associated reservoirs.

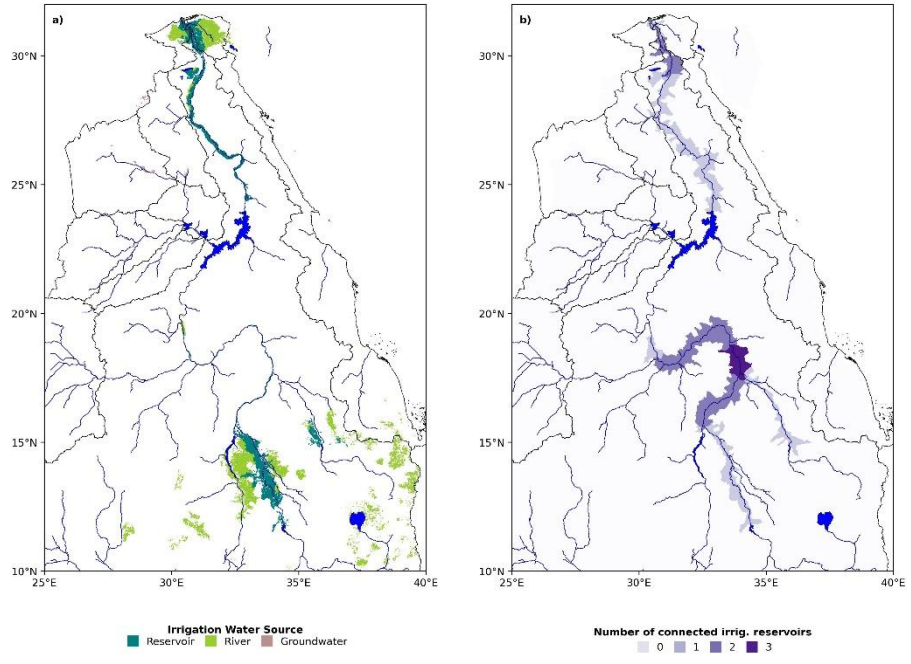

Figure 3: Example of definition of a) sources of irrigation water for agricultural, irrigated HRUs, and b) Sub-basins where HRUs can demand water to reservoirs based on irrigation topology, for a downstream section of the Nile River and adjacent basins in CoSWAT.

https://doi.org/10.5194/egusphere-2026-881
Preprint. Discussion started: 5 March 2026

Finally, land use management decision tables were established for each identified HRU. For irrigated HRUs with a groundwater source, irrigation water was allowed to be extracted from the shallow aquifer. For those with a surface-water source, water was extracted from the nearest river to the HRU. In all cases, irrigation is applied based on a water-stress threshold rather than a fixed calendar. For those that require water from a reservoir, an additional land use management action was implemented in the SWAT+ source code to record reservoir irrigation water demand. This means that water is not directly extracted from the reservoir; only the demand is recorded, which influences the reservoir's release.

2.6 Simulation setup, model comparison, and evaluation

The model was configured for the 9 selected regions using spatial input data at 0.01° resolution, finer than the 0.02° resolution of CoSWAT v1(Chawanda et al., 2025). The weather forcings were derived from the GSWP3-W5E5 dataset, and the simulations were conducted using the adjusted version of SWAT+ (revision 61.0.2) at a daily time step for the period 1965-2015, with a 5-year warm-up. The initial storage for all water bodies was set to their principal volume. The model outputs were evaluated using Kling-Gupta Efficiency (KGE), percent bias (PBIAS), and coefficient of correlation (r) for both streamflow and reservoir storage, as well as inflow and outflow. To assess model adequacy, thresholds were defined for these statistical performance/error indicators. Given that this is a large-scale application with coarse input data, the minimum acceptable KGE value was set to -0.42, which represents a better performance than just taking the mean of the observations (Knoben et al., 2019). However, the objective value for satisfactory performance was set at a minimum KGE of 0.0, with 0.4 considered good performance, and this was similarly applied to r. The PBIAS threshold and objective were set to ±50% as satisfactory, and ±25% as good (Moriasi et al., 2007).

2.6.1 Reservoir storage, inflow, and outflow

The model version with new implementations was evaluated for its ability to represent the monthly means of reservoir storage, inflow, and outflow. For this, the GRS (Li, 2023), ResOpsUs (Steyaert et al., 2022), and selected data by Yassin (2018), as summarized in Table 1 was pre-processed and aggregated. Only reservoirs with at least 5 years of at least 1 data point and 1 year of continuous storage data were considered, then aggregated across sources. If a reservoir had multiple data sources, the average value was used as the reference.

To place model performance in a broader context, monthly reservoir storage was compared against five state-of-the-art global water models from the ISIMIP Global Water Sector (Gosling et al., 2024): CWATM, H08, LPJmL5-7-10-fire, MIROC-INTEG-LAND, and WaterGAP2-2e. All models were evaluated using simulation outputs driven by observationally based GSWP3-W5E5 climate forcing and historical human-socioeconomic forcings for the same period as this study. ISIMIP outputs are provided on a common 0.5° x 0.5° grid, where each cell represents aggregated water storage from all lakes and reservoirs within that cell (i.e., representative water body). For each evaluated reservoir, the storage time series was extracted at the grid cell corresponding to the reservoir outlet. This differs from CoSWAT, whose outputs are not gridded and are produced explicitly for each water body. Where multiple reservoirs/lakes fell within the same grid cell, their contributions were

https://doi.org/10.5194/egusphere-2026-881
Preprint. Discussion started: 5 March 2026

proportionally weighted using their maximum recorded volume from the HydroLakes dataset. If the sampled grid cell from the ISIMIP models produced a time series of persistent zero storage, the reservoir was assumed not to be represented in that model and was excluded from further analysis.

2.6.2 Streamflow

To assess the impact on streamflow performance, the model was configured with and without the new implementations, yielding one version for each region that included lakes, reservoirs, and irrigation, and another that excluded them. What is important about this evaluation, is that the CoSWAT model has not been calibrated (Chawanda et al., 2025), so the simulations were conducted with default parameter values for relevant hydrological processes and river routing. Monthly streamflow performance, using GRDC data as the reference, was compared between the two versions at stations downstream of a lake or reservoir significantly impacted by new implementations, i.e., the absolute KGE skill score (Towner et al., 2019) is above 0.05 following Eq. (B- 1). Performance thresholds were used to assess how the new implementations affect model performance, with particular emphasis on the KGE metric. Based on them, four categories were established for comparison:

- Category 1: Performance without implementations is satisfactory (KGE > 0) and new implementations increase KGE.
- Category 2: Performance without implementation is not satisfactory (KGE < 0), and new implementations increase KGE.
- Category 3: Performance without implementations is satisfactory (KGE > 0), and new implementations decrease KGE.
- Category 4: Performance without implementations is not satisfactory (KGE < 0), and new implementations decrease KGE.

This evaluation helps identify where improvements occur or do not, and to what extent, which is especially useful when examining categories 2 and 3, as crossing the satisfactory threshold is possible. Those in category 1 represent locations where the model alone performs satisfactorily, but the new implementations further increase its reliability. In contrast, those in category 4 represent locations where poor performance has already occurred; the new implementations are initially counterproductive, while other factors are more influential and potentially more relevant for improving model performance.

3 Results

3.1 Lake and reservoir resolution into model structure

The new network-resolution process implemented in the CoSWAT-Framework integrated 498 reservoirs or lakes into the model structure for the study regions, out of 632 possible (excluding those filtered out by the initial area and degree of regulation thresholds), yielding an efficiency of 79%. Nonetheless, considering the maximum storage capacity or representative storage based on global datasets, the integrated water bodies account for 2992 km3 of storage out of 3286 km3, representing 91% of the total storage.

https://doi.org/10.5194/egusphere-2026-881
Preprint. Discussion started: 5 March 2026

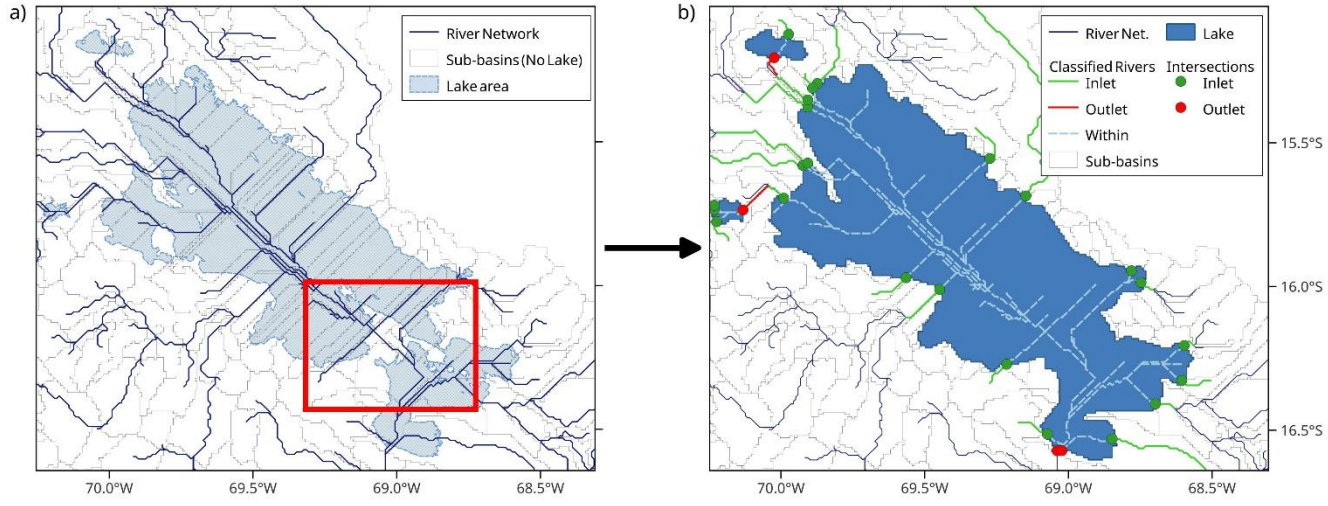

Figure 4: Example of Lake Titicaca in the model structure, a) before network resolution process, and b) after resolution, showing classified river network elements and points of intersection at the water body limits to define inlets and outlets. Rivers classified as "Within" are eventually excluded from the model structure. The area marked in red on box a) represents the Lago Menor division, an example where complex topography leads to a network in which the lake cannot be integrated without the new resolution approach.

Figure 4 shows one of the complex cases where the CoSWAT Framework would typically fail to integrate a water body into the model structure, as only river endpoint geometrical rules are not sufficient, and require a more robust approach considering network topology: Lake Titicaca, which has complex locations such as the Lago Menor division (highlighted area, box a). The resolution process simplified the geometry in the vector file. However, physical properties related to area, storage, and h-A-V relationships remain correctly represented in the model, as global dataset values are introduced in the simulation model files. This is one of many cases that showcase how the new resolution approach enables more efficient integration of water bodies.

3.2 Reservoir and lake storage, inflow and outflow evaluation

A total of 215 water bodies were evaluated for monthly storage, with results summarized in Figure 5a and Figure B- 1. In terms of KGE, 150 (70%) achieved a value above the minimum threshold (-0.42); however, only 73 (34%) achieved a positive KGE value. The distribution is approximately normal, with a median of -0.1; however, it has a long tail toward negative values, indicating fewer cases with very poor performance. Moreover, for 94 cases (44%), PBIAS was between the satisfactory ±25% range. Overall, the PBIAS distribution for storage is wide and moderately asymmetric, with extended tails toward both large negative and positive values, but with a stronger tendency toward overestimations. The correlation coefficient was positive in 153 cases (71%), with 48 stations (22%) achieving a good performance ($r > 0.4$). A large proportion of stations fall within the intermediate range (0-0.4), indicating moderate but not consistently strong model performance across sites.

https://doi.org/10.5194/egusphere-2026-881
Preprint. Discussion started: 5 March 2026

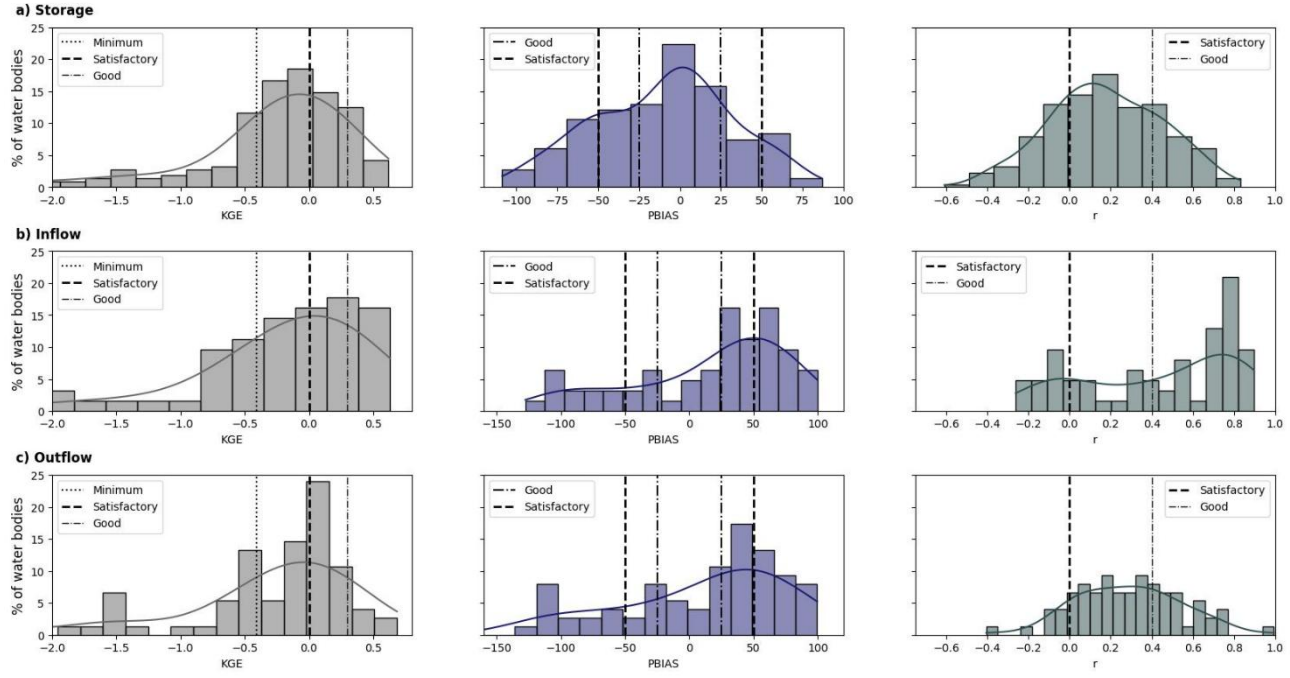

Figure 5: Distribution of KGE, PBIAS, and R related to model performance for monthly mean a) storage, b) inflow, and c) outflow, using normalized histograms expressed as a percentage of evaluated water bodies for the corresponding variable. A kernel density estimate (KDE) curve is overlaid on each histogram to provide a continuous representation of the underlying probability distribution. Vertical reference lines indicate the established adequacy classifications for performance thresholds.

Monthly inflow performance was assessed for 62 water bodies, and outflow for 75 (Figure 5b and Figure 5c, respectively). For inflow, in 44 cases (71%), the minimum KGE threshold was exceeded, but fewer than half (28 sites) achieved a positive value. The inflow KGE distribution is centered near zero, with a long tail toward very poor performance. Only 11 cases (18%) had inflow PBIAS in the satisfactory range; there is widespread over- and underestimation, with a high concentration of cases around moderate positive biases and a significant number of important overestimations. Outflow performance is generally similar: 49 sites (65%) exceed the minimum KGE threshold, but only 27 achieve a positive KGE. Outflow shows even greater PBIAS variability, driven mainly by several extreme biases. Correlation is predominantly positive for both variables, but consistently higher for inflow (60% of stations above 0.4) than for outflow (33% above 0.4), suggesting that the model generally captures inflow timing better than outflow timing.

To further explore the drivers of storage performance, relationships among storage metrics, inflow/outflow skill, and water body characteristics were analyzed (Figure B- 2). Storage KGE shows a moderate to low, statistically significant positive relationship with inflow and outflow KGE ($r \approx 0.35$ - 0.38), indicating that improved representation of inflows is associated with better storage and outflow performance, particularly for reservoirs exceeding the minimum skill threshold for storage (KGE > -0.42). A similar pattern is observed for inflow timing: higher storage performance is associated with higher inflow correlation ($r \approx 0.39$), suggesting that improvements in the temporal representation of inflows yield more realistic storage

https://doi.org/10.5194/egusphere-2026-881
Preprint. Discussion started: 5 March 2026

dynamics. In addition, storage PBIAS shows a moderate-to-low relationship with elevation ($r \approx 0.32$); however, a clear cluster of reservoirs at lower elevations (500 masl and below) exhibits substantial negative biases, suggesting that the model overestimates storage in downstream regions.

To illustrate the representation of reservoirs and lakes Figure 6 compares simulated and reference storage, inflow, and outflow for three water bodies with sufficient data availability on different orders of magnitude in terms of their storage capacity. Overall, storage performance is satisfactory for these three cases, while inflow and outflow skills vary and are better understood through graphical assessment of the time series. Berryessa Lake (Figure 6a) is a regulated water body mainly used for hydroelectricity, and shows the best overall performance: storage is well reproduced except for notable underestimation during 1999-2004. Inflow is temporally consistent but generally underestimated, whereas outflow has a reasonable magnitude and PBIAS, but has timing errors, with simulated peaks occurring earlier (January) than observed (February-March). This example highlights that a good outflow estimation may not always accompany a good reservoir storage representation.

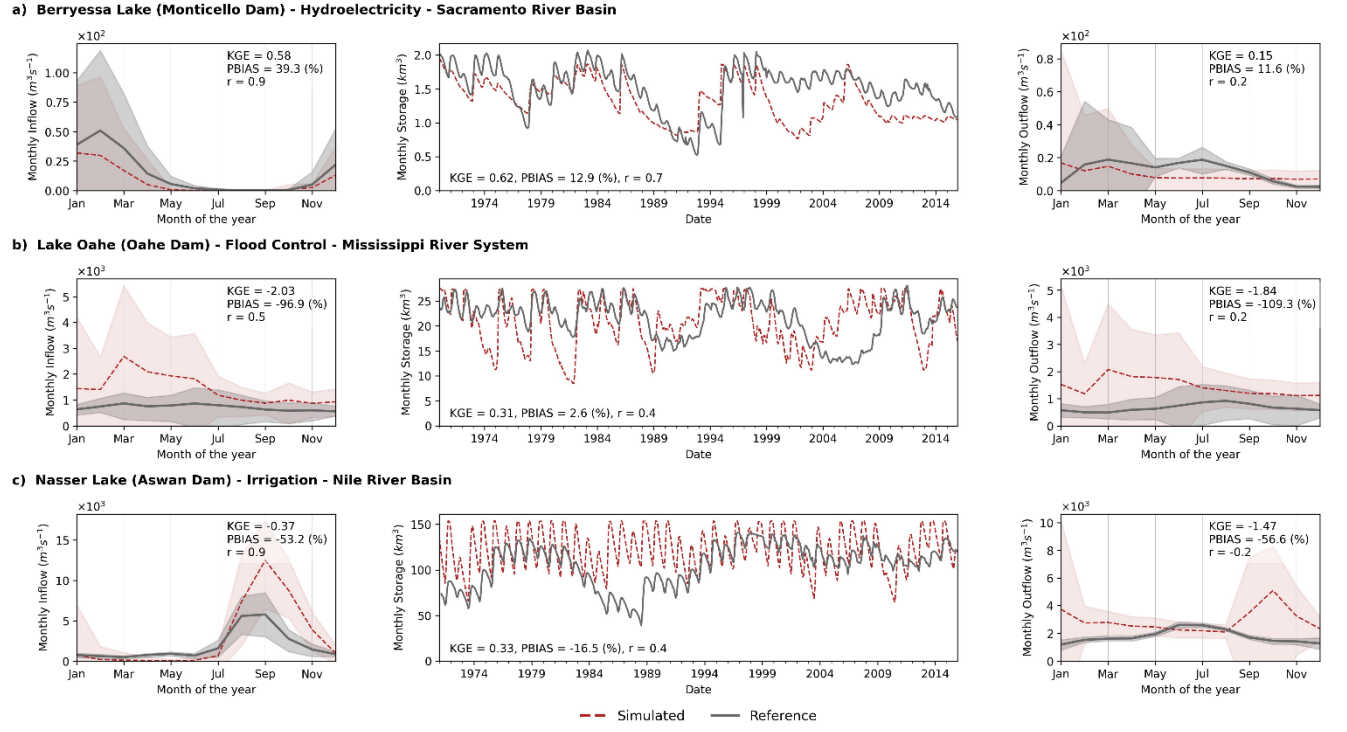

Figure 6: Simulated and reference data comparison for monthly inflow climatology (left), monthly storage (center), and monthly outflow climatology (right) on 3 selected water bodies: a) Berryessa Lake, b) Lake Oahe, c) Nasser Lake. Shaded bands in plots for seasonal monthly inflow/outflow show the mean ± 1.5 times the standard deviation.

Lake Oahe (Figure 6b) primarily operated for flood control, attains a satisfactory KGE and reasonable average storage magnitude, yet exhibits frequent storage underestimations that result in larger variability than observed. This behavior is linked to poor inflow and outflow timing and general overestimation of their magnitudes; inaccurate inflow representation propagates

https://doi.org/10.5194/egusphere-2026-881
Preprint. Discussion started: 5 March 2026

into excessive releases and consequently degrades storage performance. A comparable pattern is observed for Lake Nasser (Figure 6c), an irrigation-oriented reservoir, where storage is often overestimated and its variability exaggerated. Moreover, in the period 1984-1994, a significant drop in storage was not captured. Although inflow timing is relatively well represented, magnitudes are generally too high, while outflow is both overestimated and temporally shifted. Based on reference data and other reports (Abdellatif et al., 2025), the Aswan Dam in Nasser Lake releases up to 60 km^3 $year^{-1}$, mainly for irrigation. Throughout the year, the model tends to overestimate the release, yet the simulated irrigated amount downstream averaged 7-10 km^3 yr^{-1}, indicating a substantial underestimation of irrigation demand. Hence, there is a combined effect of overestimating surface runoff and misrepresenting irrigation demand in both magnitude and timing.

3.3 Comparison with other global models

As an additional benchmark for the storage evaluation, results were compared with five global water models from the ISIMIP Global Water Sector. Across these models, the number of reservoirs evaluated varies widely, from 65 for CWATM to 195 for LPJmL5-7-10-FIRE, with intermediate sample sizes for H08 (78), MIROC-INTEG-LAND (183), and WaterGAP2-2e (96). In contrast, CoSWAT results encompass 197 water bodies, effectively covering the union of those represented across all models. These differences arise because grid cells with all-zero storage time series were excluded, suggesting that the reservoir is not represented in the model or that the sampled pixel does not precisely match its location. Accordingly, the performance distributions shown in Figure 7 are computed using only the subset of water bodies simultaneously represented by CoSWAT and each respective ISIMIP model, so the CoSWAT sample size varies per comparison rather than always including the full set of 197 reservoirs. In contrast, the bar charts reporting the proportion of water bodies exceeding performance thresholds are normalized by the total number of reservoirs represented by each model, thereby reflecting overall coverage and skill. Given these differences in sample size and normalization, inter-model comparisons should be interpreted as indicative benchmarks relative to CoSWAT rather than definitive global performance assessment of the five ISIMIP Global Water models.

Overall, the models show broadly comparable storage skill, as indicated by median KGE values clustering from weakly negative to slightly positive. CWATM obtains the highest median KGE (0.10), followed by WaterGAP2-2e (-0.08), and H08 (-0.11), while MIROC-INTEG-LAND (-0.44), and LPJmL5-7-10-FIRE (-0.56) exhibit progressively lower medians, below the -0.42 threshold. For the 197 water bodies, CoSWAT achieves a median KGE of (-0.08), although this varies by subset with direct comparisons. The violin plots reveal variability across all models, with notable differences in spread: CWATM shows the most compact interquartile range and KDE curve, whereas LPJmL5-7-10-FIRE and H08 display broader distributions with long tails towards negative KGE values. CoSWAT, WaterGAP2-2e, and MIROC-INTEG-LAND are comparable in their variability, which is somewhat moderate. However, the two former show interquartile ranges centred on higher KGE values than the latter. Regarding performance thresholds, CWATM has the highest number of water bodies with satisfactory KGE (62%), followed by WaterGAP2-2e (44%), CoSWAT and H08 (both ≈ 40%), with the rest below 25%. WaterGAP2-2e and H08, however, achieve the highest proportion of water bodies with a “good” performance (KGE > 0.4) with approximately 20% and 16%, respectively, while for the rest, this is below 10%.

https://doi.org/10.5194/egusphere-2026-881
Preprint. Discussion started: 5 March 2026

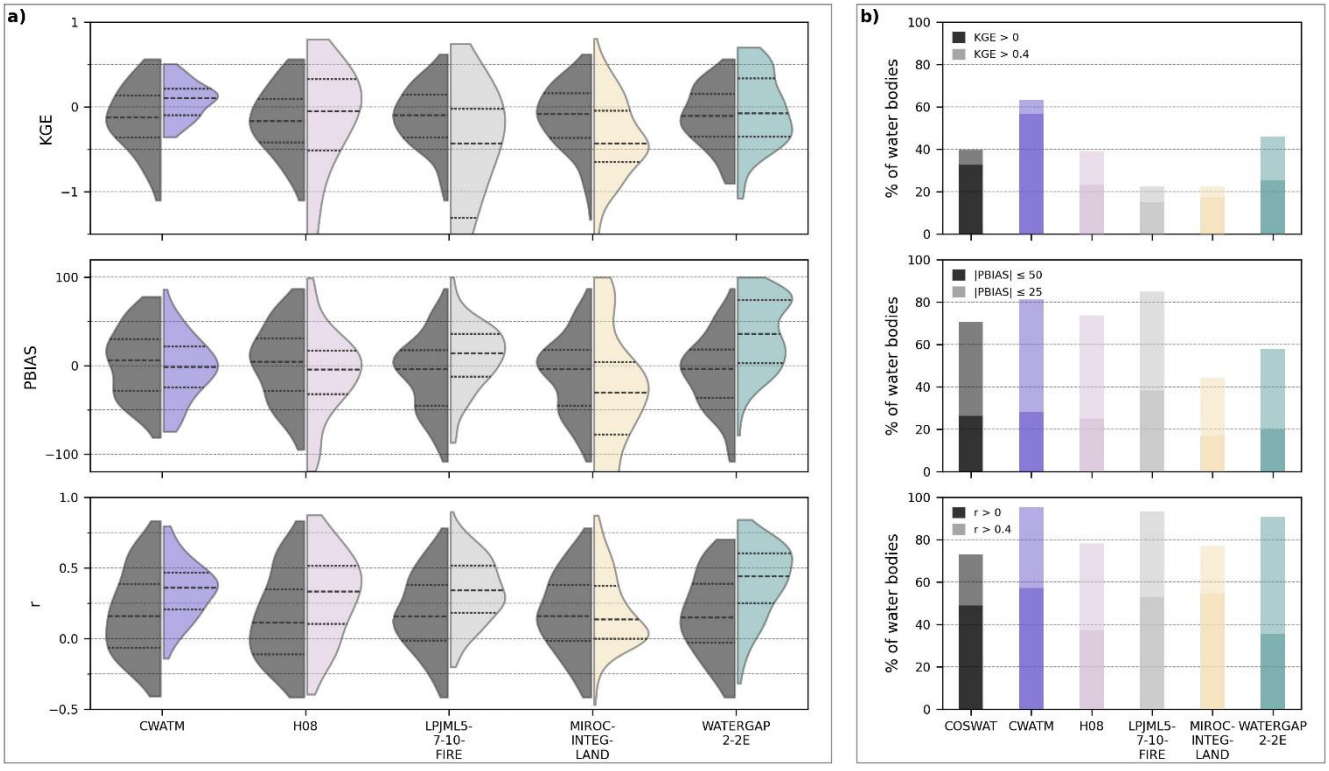

Figure 7: Performance comparison for mean monthly storage representation between CoSWAT with new implementations and five ISIMIP Global Water Sector models. Box a) shows violin plots with the KDE distribution of CoSWAT (left) and the other models (right) for KGE, PBIAS, and r, considering only the water bodies available in the ISIMIP reference model. A dashed line represents the median, while dotted lines represent the first and third quartiles. Box b) shows the percentage of water bodies per model that are above the "satisfactory" and "good" threshold for its corresponding performance/error index. Outliers were not considered.

For PBIAS, CWATM, CoSWAT (across 197 bodies), and H08 are closest to zero (median PBIAS of -1.2%, -3.9%, and -4.1%, respectively), whereas MIROC-INTEG-LAND and WaterGAP2-2e display much stronger median biases (-30% and +36%), indicating a general over- or under-estimation. The PBIAS distributions are broad across all models, particularly for MIROC-INTEG-LAND, which exhibit extensive ranges and multiple extreme values. The PBIAS KDE curve is relatively centred around zero for CWATM, H08, and CoSWAT, in contrast to the others, though it remains spread. Most models achieve satisfactory PBIAS at at least half of the stations, except for MIROC-INTEG-LAND, which achieves only about 43%. For the coefficient of correlation, WaterGAP2-2e achieves the highest median value (0.43), followed by CWATM (0.35), LPJmL (0.34), and H08 (0.30), while CoSWAT (0.16) and MIROC-INTEG-LAND (0.13) show weaker correspondence in temporal variability. The distribution of r for CoSWAT shows a large proportion above 0; the density is high around values below 0.2, and it also has the lowest proportion of water bodies with an r value above 0.4 (73%).

https://doi.org/10.5194/egusphere-2026-881
Preprint. Discussion started: 5 March 2026

3.4 Streamflow evaluation

A total of 192 stations were identified as significantly affected by the new implementations, and model performance was evaluated for these stations both with and without the new implementations. Across all stations, the median KGE increased from -0.07 to 0.05 following the new implementations. The number of stations with a good performance increases from 49 (25%) to 58 (30%), while the number of stations with satisfactory performance (KGE > 0) remains similar (44 to 40), and the stations surpassing the -0.42 threshold increase from 23 (12%) to 32 (17%). Overall, following the new implementations, the percentage of stations that meet the minimum threshold increases from 60% to 68%. In terms of PBIAS, the median value is reduced from -24% to -16%, and the number of stations within the satisfactory range (±50%) increases from 50 (26%) to 57 (29%). The coefficient of correlation was above 0.4 at 152 (87%) stations with new implementations, compared with 159 (85%) without them. Overall, the observed changes based on the number of stations within a certain threshold are sometimes modest, highlighting the importance of looking at them in terms of the absolute change in performance indicators within their corresponding skill category (Figure 8). Most stations fell into categories where skill increased with new implementations: 80 stations (42%) were initially poor and improved (Category 2), and 53 (28%) were already acceptable and improved further (Category 1). Conversely, 19 stations (10%) declined in skill from an initially poor state (Category 4), and 40 (20%) showed reduced skill despite initially acceptable performance (Category 3). Only a small fraction of stations crossed the KGE sign: 11 stations in Category 2 flipped from negative to positive, while 6 in Category 3 flipped from positive to negative. Regarding the minimum threshold (KGE > -0.42), 19 stations in Category 2 crossed above this limit, whereas only 2 in Category 3 crossed below it; 49 stations in Category 2 remained below the threshold, clearly showing that improvements achieved by the current integration of reservoirs and lakes are not directly leading to surpassing performance thresholds in most stations.

Spatially (Figure 8, box a), Category 3 stations cluster in the lower Mississippi River system, particularly in downstream reaches with extensive drainage areas, reflecting the trade-off associated with new implementations; however, in most of these stations, performance remains above satisfactory levels. A very common situation is what can be observed in the upper Mississippi River System, overall in the Colorado River Basin, Nile River Basin and most sections of Western Europe: many stations are improving (Category 2), yet their KGE value remains below the minimum threshold, a clear indication that new implementations alone are not sufficient to take performance to satisfactory levels, but an improvement is indeed achieved. In Central Europe, a large number of stations are classified as Category 1 or 2, and, as with the stations mentioned earlier, most of those in Category 2 remain below the satisfactory threshold. There are also a significant number of Category 3 and 4 stations, with the former remaining satisfactory in KGE despite reductions. The Parana and Titicaca River Basins in South America have relatively few observations compared with the aforementioned regions, and the results vary significantly. Upstream stations are generally classified as Category 1 or 2, and we again observe that the latter remain below satisfactory levels. A small number of midstream stations show a reduction in KGE, but their performance remains good. All stations in the downstream of the Parana Basin have Category 4. In the Orange Basin of southern Africa, results are generally varied, and categories are distributed equally. What is clear is that although some upstream stations continue to perform poorly, the

https://doi.org/10.5194/egusphere-2026-881
Preprint. Discussion started: 5 March 2026

majority of mid- and downstream stations achieve satisfactory levels, with a mix of improvements and reductions in KGE. The Mekong River Basin has the fewest affected stations, classified as Category 3 and Category 1; the majority remain above satisfactory levels following implementation.

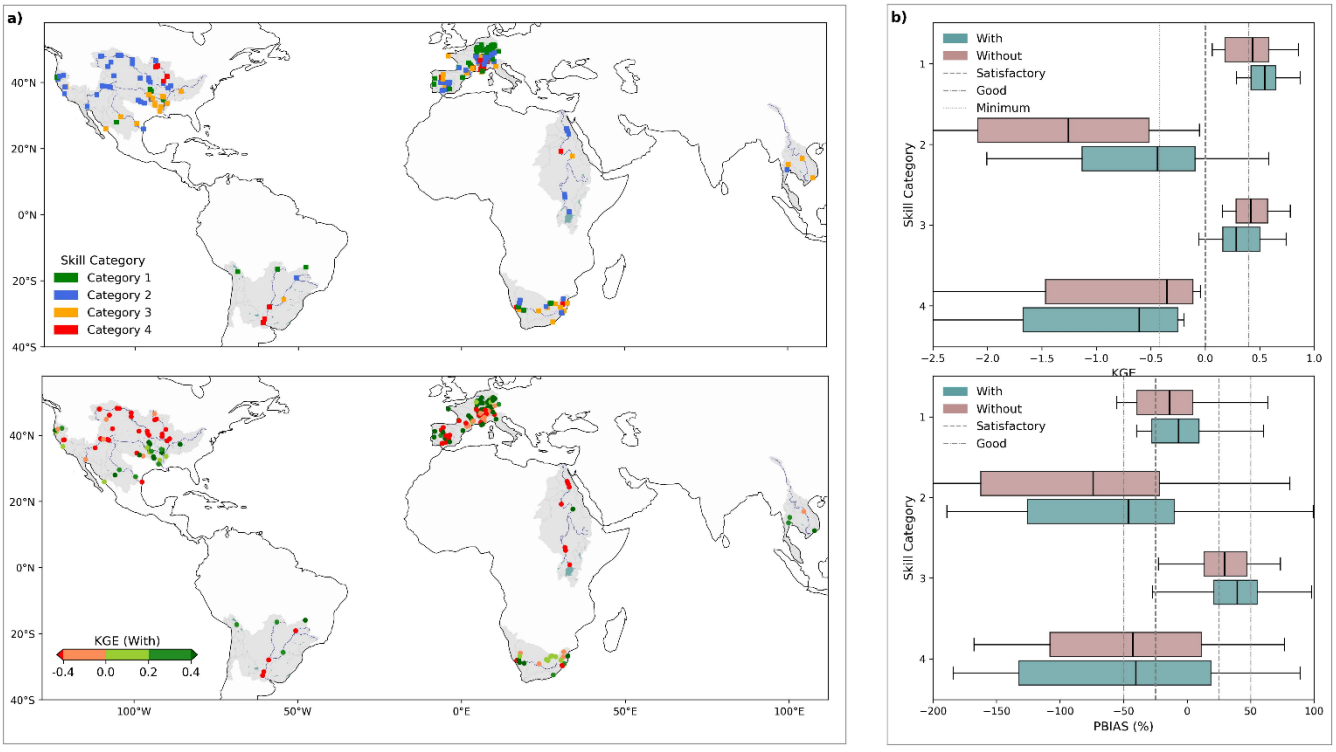

Figure 8: Monthly streamflow performance assessment. Box a) shows the spatial distribution of stations with their corresponding skill category (top) and the KGE value of the model with new implementations (bottom). Box b) shows the distribution of performance per skill categories for KGE (top) and PBIAS (bottom) with and without new implementations, as well as the performance classification thresholds.

The box plots (Figure 8, box b), indicate that stations that were already performing well show an important improvement (Category 1), with a positive shift in the median for both KGE and PBIAS, leading to a majority of stations achieving good performance and a better PBIAS. The KGE distribution for stations in Category 3 shows that, despite reductions, the majority remain satisfactory; however, with respect to PBIAS, there is a general shift towards large positive values, indicating a tendency to overestimate (i.e., likely to over-represent reservoir regulation). Category 2 shows the largest changes, with a substantial increase in the mean KGE from -1.3 to -0.43 and a distribution generally closer to satisfactory levels, although, as noted earlier, still with a majority below the desired values. In this category, there is a clear tendency to overestimate, with the PBIAS distribution concentrated in negative PBIAS values; this tendency is mitigated by recent implementations, which shift the mean toward the satisfactory range. Nevertheless, this highlights that the underlying issue leading to poor performance at these stations may be an overestimation of surface runoff. Finally, we observe a significant reduction in Category 4 stations, with KGE decreasing further and the PBIAS distribution expanding.

https://doi.org/10.5194/egusphere-2026-881
Preprint. Discussion started: 5 March 2026

To illustrate how reservoir implementation affects streamflow behavior, six representative stations were selected to capture the range of positive and negative responses to new implementations (Figure 9). The plots show the climatology of monthly mean streamflow, with ±1.5 standard deviations, enabling direct comparison of variability and extremes. Overall, the examples demonstrate that the inclusion of water bodies as reservoirs and lakes can moderate seasonal dynamics in many basins but can also introduce new biases depending on how releases or outflows are represented.

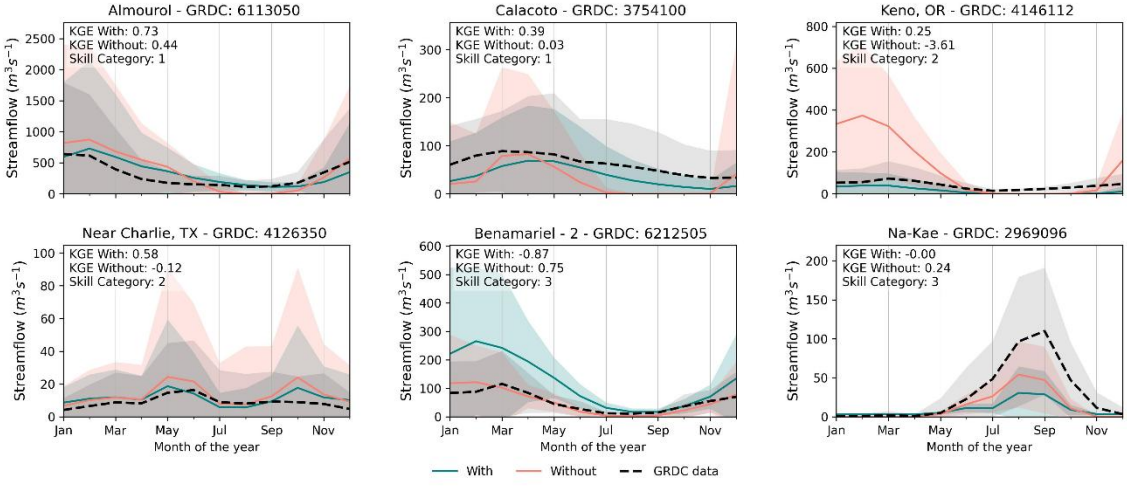

Figure 9: Seasonal monthly streamflow patterns for six selected GRDC stations, contrasting simulations with and without new implementations. Lines show the mean monthly flow across the analysis period, while shaded bands denote ±1.5 standard deviations. Titles indicate the GRDC station number and ID.

In the first three cases (Almourol, Calacoto, and Keno), improved performance is primarily associated with reduced extremes and more realistic dry-season flows, consistent with the regulating effect of reservoirs. In particular, the Keno station clearly illustrates how the absence of upstream water bodies leads to unrealistically high flows, thereby shifting KGE from negative to positive. The fourth case (Near Charlie, TX) primarily reflects a reduction in the overly high peaks observed in the no-reservoir simulation. In contrast, the fifth station (Benamariel) shows a situation where reservoirs increase simulated flows because their releases are overestimated, while the sixth case (Na-Kae) exhibits the opposite behavior, with reservoir or lake outflows that are too low, leading to significant underestimation of seasonal flows: a clear case of over-representation of reservoir disruptivity combined with a general underestimation of surface runoff and streamflow.

4 Discussion

4.1 Integration of lakes, reservoirs, and irrigation

The representation of lakes and reservoirs in the SWAT+ model structure posed a topological challenge that was successfully addressed through improvements to the CoSWAT Framework, making it now feasible for the global CoSWAT model. Complex cases with multi-branch connections, lake or reservoir chains, and ambiguous connectivity were addressed correctly.

https://doi.org/10.5194/egusphere-2026-881
Preprint. Discussion started: 5 March 2026

The Lake Titicaca example illustrates this: a large water body with many inlets that acquires a complex geometry due to division into the Lago Menor section, which, through our process, was successfully added to the model network. Our topology-aware, robust approach, leveraging upstream-downstream connectivity and intersection logic, provided a consistent way to identify inlets and outlets and to adjust the routing network accordingly. Across the 9 model regions studied, satisfactory performance was achieved in feature integration and the hydrologic relevance of these water bodies. About 79% of candidate water bodies across all regions were successfully integrated into the network. More importantly, 91% of the total storage was represented, something as important as just the number of features, as larger water bodies will generally have a stronger influence on the basin's hydrology because of their high degree of regulation and evaporation rates (Shrestha et al., 2024; Zhao and Gao, 2019), particularly in the global context of this study.

Beyond improving the structural integration of water bodies, the automated definition of irrigation application and demand within the CoSWAT Framework addresses another key limitation of the CoSWAT Global Model: water allocation and demand (Chawanda et al., 2025). By explicitly identifying irrigated HRUs, assigning their water sources, and allowing water demand to condition reservoir release, the framework introduces a more realistic representation of agricultural water dynamics, which is essential in global modelling efforts (Haddeland et al., 2014; Pokhrel et al., 2016). Nevertheless, irrigation water demand and crop growth were not independently validated in this study, which introduces uncertainty about the realism of this component in the evaluated outputs. In addition, planting and harvesting dates follow the default SWAT+ heat-unit-based approach, which is inadequate in many regions, particularly where cropping cycles are primarily controlled by water availability rather than temperature (Nkwasa et al., 2022a). The new irrigation-reservoir linkage improves consistency and represents a significant methodological advancement for the CoSWAT model in demand and allocation, yet the representation of actual crop growth and irrigation remains limited.

4.2 Model performance of simulated reservoirs and lakes

Overall, reservoir and lake storage performance shows moderate skill, with substantial variability across river basins, as expected for large-scale models under generalized parametrizations and, as in CoSWAT, with uncalibrated parameters. Based on our comparison with other global water models, and the range of performance reported in similar large-scale evaluations (Hosseini-Moghari and Döll, 2025; Tang et al., 2025; Vanderkelen et al., 2022). The obtained storage skill is broadly comparable in magnitude and spread, indicating that the new implementations yield results as reliable as those of other state-of-the-art models. The model achieves a meaningful representation of storage dynamics, despite its uncalibrated status for hydrological processes and without requiring site-specific calibration in many cases. As expected and consistent with other global applications, KGE median values remain generally low, but a substantial fraction exceed minimum skill thresholds, with many cases achieving a satisfactory PBIAS.

An important insight arises from the observed relationship among storage, inflow, and outflow performance. The positive correspondence between storage KGE and both inflow KGE and inflow correlation indicates that the performance of the

https://doi.org/10.5194/egusphere-2026-881
Preprint. Discussion started: 5 March 2026

applied approach is strongly constrained by upstream hydrology. When inflows are reasonably well represented in terms of timing and magnitude, storage dynamics are generally simulated more realistically; however, deficiencies in inflows may propagate into storage errors. There is also a moderate correlation between storage and outflow KGE, but this is again driven by the accurate representation of inflows, particularly when the Hanasaki et al. (2006) scheme was used, as inflows directly drive the release estimates. Nevertheless, there are cases in which, despite adequate representation of inflows and storage, outflows are not, which is an expected trade-off common to methods with global applicability. The general influence that inflow representation exerts on the model's ability to represent the storage of these water bodies suggests that, prior to any reservoir-specific calibration of scheme parameters, improving the hydrological representation at the basin scale (i.e., water balance) is likely to provide a more robust pathway that can improve multiple elements. Nevertheless, particularly in regulated systems with cascading water bodies, downstream inflows are shaped by upstream regulation (Shin et al., 2019; Vanderkelen et al., 2022), which may necessitate site-specific calibration. Moreover, the Nasser Lake and Lake Oahe examples (Figure 6) clearly show that the simulation scheme is highly sensitive to inflow representation, with overestimation of inflow leading to misrepresentation of storage and outflow.

Inflow alone does not fully explain the dynamics in storage representation. In many regulated systems, reservoirs may also be strongly influenced by consumptive and non-consumptive water demands, i.e., hydroelectricity (Shrestha et al., 2024). However, the extent to which these demands are adequately represented in the present framework remains uncertain, as irrigation withdrawals were not directly validated and other demand types were not explicitly modeled. This is also exemplified by the Nasser Lake example (Figure 6), in which irrigation demand was likely underestimated and timing misrepresented. Likely because the irrigation application rules only followed the heat-unit approach for plant growth and consequently irrigation, possibly missing the actual crop calendar in the region, and therefore introducing another error in the seasonality of reservoir outflows on top of the overestimated inflows. Additionally, in this case, the general overestimation of hydrological processes, along with uncertainties in weather forcings, is also significant, as the model was unable to capture a dry period during which storage declined significantly, likely due to overestimated runoff and therefore inflow to the lake. Furthermore, the observed tendency toward stronger storage biases at lower elevations suggests that errors accumulate in downstream parts of large river systems, where increasing drainage areas and the presence of multiple upstream reservoirs amplify upstream inaccuracies, something that could be addressed by large-scale calibration approaches such as Hydrological Mass Balance Calibration (HMBC; Chawanda et al., 2020). Additionally, on large lakes and reservoirs with extensive surface areas, evaporation losses can represent a dominant component of the water balance and therefore greatly influence storage (Pillco Zolá et al., 2019; Vanderkelen et al., 2018). Although evaporation is represented in the model, its role and simulation reliability were not explicitly evaluated in our study; such an assessment could further enhance the model for these systems.

4.3 Impacts on streamflow representation

Overall, streamflow performance across all evaluated stations remains highly variable, with a wide range of skill levels and persistent biases at many locations. Such heterogeneity is common in large-scale and global hydrological models, where

https://doi.org/10.5194/egusphere-2026-881
Preprint. Discussion started: 5 March 2026

limitations related to coarse or uncertain input data, biased weather forcings, simplified process representations, and the absence of site-specific calibration generally result in lower performance compared to local applications (Abbaspour et al., 2015; Gudmundsson et al., 2021; Kumar et al., 2022). Against this background, the inclusion of lakes and reservoirs generally improves simulated streamflow performance (70% of stations), with a large portion performing poorly (42%), seeing clear and considerable increments in KGE and reductions in PBIAS, whereby reservoir or lake presence primarily affects specific aspects of the hydrograph, such as sustaining low flows and attenuating peaks (Biemans et al., 2011). Nevertheless, the performance of most of these cases, even with improvements, remains poor, suggesting that adjustments to fundamental hydrological processes are still required. In that sense, our results show a clear clustering of poorly performing stations in which streamflow overestimation occurs, suggesting a need to correct this bias by adjusting parameters associated with surface runoff generation, which HMBC could again address.

A remaining challenge is the presence of large biases in simulated reservoir outflows, which directly affect downstream streamflow performance. In many cases, improvements in streamflow associated with reservoir representation are offset by inaccuracies in release magnitude or timing. Improving the representation of reservoir releases, most likely through site-specific optimization of reservoir scheme parameters, could therefore lead to additional gains in streamflow performance (Dang et al., 2020; Shin et al., 2019). However, such improvements are not straightforward, as adjustments that reduce outflow biases may introduce trade-offs with storage dynamics, for example, by degrading the temporal variability or magnitude of simulated storage (Yassin et al., 2019). This highlights the need for approaches that jointly target catchment hydrology and reservoir behavior, rather than optimizing individual components in isolation while accepting performance trade-offs.

4.4 Implications and future work

This study highlights that improving the structural representation of lakes, reservoirs, and their connectivity is a necessary step toward more realistic global hydrological simulations in the CoSWAT model, but it must be followed by further improvements. The model shows clear benefits where reservoir influence is relevant, particularly in regulating seasonal flows, yet significant variability and biases persist across regions. This confirms that, at a global scale, reservoir and lake representation should be viewed as part of an integrated modeling framework, where gains depend on the combined quality of inflow simulation, routing, and storage dynamics. With these methodological advances, the CoSWAT model offers a robust representation of lakes and reservoirs, enabling its application in global studies to assess the impacts of anthropogenic climate change on water body storage and their implications for water availability, as well as to explore trade-offs of adaptation measures such as the construction of new dams in combination with land use and management practices. In addition, CoSWAT can be coupled with dedicated lake models to evaluate future changes in lake ecosystem health, supported by the semi-distributed structure of SWAT+, which explicitly represents individual lakes and reservoirs rather than aggregated water bodies, providing a strong basis for model coupling and aligning with the needs of initiatives such as the ISIMIP Lake Sector while remaining flexible enough to support the Global Water Sector. The CoSWAT Framework further enhances applicability across scales by enabling model configurations for selected regions using higher-resolution input data. At the same time, the new SWAT+ lake and

https://doi.org/10.5194/egusphere-2026-881
Preprint. Discussion started: 5 March 2026

reservoir implementations remain suitable for regional and local studies where detailed operational data are unavailable and generalized approaches are required.

The CoSWAT model remains uncalibrated, and despite the new improvements described in this study, performance results exhibit substantial variability, underscoring the need for further improvements. Given the computational cost of a full, site-specific streamflow calibration at the global scale, a key next step is to apply HMBC to reduce biases in the overall water balance. Such an approach has the potential to improve inflow magnitude and general streamflow behavior, and may also help reduce storage biases observed in downstream and lowland regions. Nonetheless, for a limited number of large and highly influential water bodies, a targeted, standalone calibration of reservoir scheme parameters may be pursued to complement large-scale approaches. Future work should also explicitly address large lakes and reservoirs with extensive surface areas, where evaporation can dominate the water balance and strongly control storage dynamics, thereby influencing downstream hydrology. Moreover, an improved representation of agricultural water practices is of utmost importance following large-scale approaches (Nkwasa et al., 2022a). Finally, integration of these water bodies should be translated to the water quality version of the model (Nkwasa et al., 2025), enabling global simulations of sediment and nutrient loading to lakes and reservoirs with a more complete representation of inland water bodies.

5 Conclusion

This study introduces methodological advances to improve the representation of lakes, reservoirs, and irrigation in the CoSWAT Framework and the global CoSWAT model. A new network-resolution approach, irrigation representation, and globally applicable reservoir and lake schemes that combine the capabilities of SWAT+ with state-of-the-art approaches used in global models were implemented. These developments enable the explicit representation of individual water bodies and their interactions with the river network, thereby improving the structural consistency of large river basin simulations.

Simulations were performed to assess the model's capability with and without the new implementations. The evaluation shows that storage dynamics are simulated with performance comparable to other global water models, and that streamflow performance improves at many stations where reservoir influence is relevant, particularly through better regulation of seasonal flows, including low- and high-flow conditions.

Overall, the results demonstrate that improved representation of inland water bodies is a necessary step toward more realistic global hydrological simulations and enables more complete, reliable, and robust global studies. The CoSWAT Framework provides a strong basis for future developments and applications across multiple scales, while the semi-distributed structure of SWAT+ remains a key strength of the model. At the same time, the limitations inherent to global modelling persist, highlighting the need for continued efforts, including large-scale calibration, improved representation of evaporation, water demands, agricultural practices, and the integration of water quality components.

https://doi.org/10.5194/egusphere-2026-881
Preprint. Discussion started: 5 March 2026

Code and data availability

The input data required to set up the model, the processed reference datasets used for model evaluation, and the post-processed simulation outputs for the nine CoSWAT regions are available on Zenodo under the CC-BY-4.0 licence. The version used to generate the results presented in this paper is archived under DOI: https://doi.org/10.5281/zenodo.18733431 (Teran, 2026a).

The scripts used in this study, including those for model setup, simulation execution, post-processing, validation, and figure generation, together with a comprehensive step-by-step guide to reproduce all results presented in this manuscript, are available from https://github.com/jopator/teran_2026_coswat_reservoirs under the MIT licence. The version used to generate the results presented in this paper is archived on Zenodo under DOI: https://doi.org/10.5281/zenodo.18746130 (Teran, 2026b).

The CoSWAT-Framework used to configure regional model setups is available from https://github.com/jopator/CoSWAT-Framework under the MIT licence. The version used in this study is archived on Zenodo under DOI: https://doi.org/10.5281/zenodo.18746453 (Chawanda and Teran, 2026).

The SWAT+ source code version used in this study (including the modifications described in this paper) is available from https://github.com/jopator/swatplus under the LGPL licence. The version used in this study is archived on Zenodo under DOI: https://doi.org/10.5281/zenodo.18727784 (Arnold et al., 2026).

Complete regional model directories and raw CoSWAT simulation outputs are extremely large (multiple terabytes) and are therefore not distributed. However, the archived data repository https://doi.org/10.5281/zenodo.18733431 includes all spatial input data required to configure the model, the processed outputs necessary to reproduce all figures and results presented in this manuscript, and one fully configured example model setup (*america-bravo* CoSWAT region) demonstrating the exact structure and configuration used in this study. The documentation at https://github.com/jopator/teran_2026_coswat_reservoirs describes in detail how to reproduce the full model setup and simulations, and how to proceed with post-processing and analysis of results.

All external global datasets referenced in this study are publicly available from their respective repositories, as cited in the manuscript.

Author contributions

JPT contributed to the conceptualization, data curation, formal analysis, investigation, methodology, resources, software, visualization, writing of the original draft, and edition of the manuscript. CJC contributed resources, software, review, and editing of the manuscript. AN, IV, and JGA contributed to the review and editing of the manuscript. AVG contributed to the conceptualization, funding acquisition, supervision, and the review and editing of the manuscript.

https://doi.org/10.5194/egusphere-2026-881
Preprint. Discussion started: 5 March 2026

Competing interests

The authors declare that they have no known competing financial or personal interests that could have influenced the work reported in this paper.

Acknowledgements

The authors wish to acknowledge the Research Foundation – Flanders (FWO) funded International Coordination Action (ICA) “Open Water Network: impacts of global change on water quality" (project code G0ADS24N) and the AXA Research Fund supporting the AXA Research Chair on Water Quality and Global Change.

https://doi.org/10.5194/egusphere-2026-881
Preprint. Discussion started: 5 March 2026

Appendix A. Details on new lake and reservoir simulation approach

Default water body evaporation and groundwater seepage calculations

Following Neitsch et al. (2011), in SWAT+, evaporation from a water body is estimated as:

$$E = \eta \cdot E_o \cdot SA \quad \textbf{(A- 1)}$$

Where E (m^3 day^{-1}) is the volume of evaporated water, η is an evaporation coefficient fixed at 0.6, E_o (m) is the potential evapotranspiration water column equivalent estimated based on weather variables, and SA (m^2) is the surface area of the water body.

The seepage to groundwater is estimated based on:

$$G = K_{sat} \cdot SA \quad \textbf{(A- 2)}$$

Where G (m^3 day^{-1}) is the volume of infiltrated water, K_{sat} (m day^{-1}) is the saturated hydraulic conductivity of the soil at the bottom, and SA (m^2) is the surface area of the water body.

Parametric, time-variant, retrospective reservoir release scheme

The H06 scheme distinguishes between two types of reservoirs for determining the release estimation approach (Hanasaki et al., 2006): non-irrigation and irrigation. Therefore, we implement the non-irrigation approach for reservoirs whose primary uses are water supply, flood control, or hydroelectricity; the other approach is applied to irrigation-purpose reservoirs. Moreover, this scheme applies the concept of operational years, which does not follow the calendar year, but is unique to each reservoir and depends on the seasonal changes in storage: the operational year starts the first day of the month in which the average multi-year inflow drops below the mean annual inflow of the last year of the simulation. At the beginning of each month of the operational year, a monthly release target is established. For non-irrigation reservoirs:

$$Q_{target} = I_{mean} \quad \textbf{(A- 3)}$$

where I_{mean} (m^3 s^{-1}) is the mean monthly inflow of a determined number of past years.

For irrigation reservoirs:

$$Q_{target} = \begin{cases} (1-\beta) \cdot i_{mean} + \beta \cdot I_{mean} \left(\frac{d_{mean}}{D_{mean}}\right), (D_{mean} \geq \beta \cdot I_{mean}) \\ I_{mean} + d_{mean} - D_{mean}, (D_{mean} < \beta \cdot I_{mean}) \end{cases} \quad \textbf{(A- 4)}$$

https://doi.org/10.5194/egusphere-2026-881
Preprint. Discussion started: 5 March 2026

where i_{mean} (m^3 s^{-1}) is the mean inflow of the last month, D_{mean} (m^3 $month^{-1}$) is the mean monthly irrigation water demand of a determined number of past years, d_{mean} (m^3 $month^{-1}$) is the mean irrigation water demand of the last month, and β is a coefficient representing environmental flow requirements; in this application, it was taken equal to 0.9, ensuring 10% of I_{mean} as environmental flow under normal conditions (Biemans et al., 2011; Vanderkelen et al., 2022).

The next component necessary to estimate the reservoir release is the release coefficient:

$$k_{rls} = \frac{S_{ini}}{\alpha \cdot S_{max}}$$

(A- 5)

where S_{ini} (m^3) is the reservoir storage at the beginning of the operational year, S_{max} (m^3) is the maximum storage capacity, here taken as the Emergency Volume, and α is a scaling coefficient that quantifies the share of active storage, set to 0.85.

The release coefficient represents the reservoir's initial fill level at the start of the operational year and is used, together with the capacity ratio, to determine the actual release. The capacity ratio defines whether a reservoir is classified as multi-year or within-a-year, and can be calculated as the ratio of S_{max} over I_{mean}. A reservoir is classified as within-a-year when the capacity ratio is below 0.5, meaning that the multi-year average inflow exceeds the storage capacity before the end of the operational year; conversely, when the capacity ratio is above 0.5, the reservoir is classified as multi-year. Based on that, the actual release is calculated as:

$$Q_{out} = \begin{cases} k_{rls} \cdot Q_{target}\ , (c \geq 0.5) \\ \left(\frac{c}{0.5}\right)^2 \cdot k_{rls} \cdot Q_{target} + \left[1 - \left(\frac{c}{0.5}\right)^2\right] \cdot i\ , (c < 0.5) \end{cases}$$

(A- 6)

where c is the capacity ratio.

Central to this scheme is a retrospective approach that examines past inflows and/or irrigation demand. For our implementation in this study, we apply this concept dynamically, considering a rolling window of 60 months (i.e., 5 years) prior to the current month of the simulation, similar to Gharari et al. (2024). These variables are stored and are used to derive and update I_{mean} and/or D_{mean} every month of the simulation, meaning they are not fixed across operational years.

Changes in the SWAT+ source code

The subroutines, modules, and associated changes in the SWAT+ revision 61.0.2 source code are summarized in Table A- 1. The adjusted version was compiled with the Intel Fortran Compiler.

https://doi.org/10.5194/egusphere-2026-881
Preprint. Discussion started: 5 March 2026

Table A- 1: Summary of changes in subroutines and modules of the SWAT+ source code

Subroutine	Description	Main changes
reservoir_module	Establishment of water body objects and associated variables.	Introduced an array of N months to store past inflows and demands, capacity ratio, and operational year.
res_control	Water balance calculation of water bodies.	Introduced a loop to store past inflows in a memory array of N months for lakes and reservoirs.
res_hydro	Reservoir or lake outflow definition in connection with decision tables.	Introduced new reservoir and lake outflow parametric schemes used in this study as release options for decision tables.
res_init	Water body initialization.	Initialized new variables created in reservoir_module.
actions_module	General decision table or management schedule associated with actions.	Introduced action for HRUs to demand irrigation water to a reservoir that can condition the release.

https://doi.org/10.5194/egusphere-2026-881
Preprint. Discussion started: 5 March 2026

Appendix B. Additional results and details for model evaluation

Additional Figures

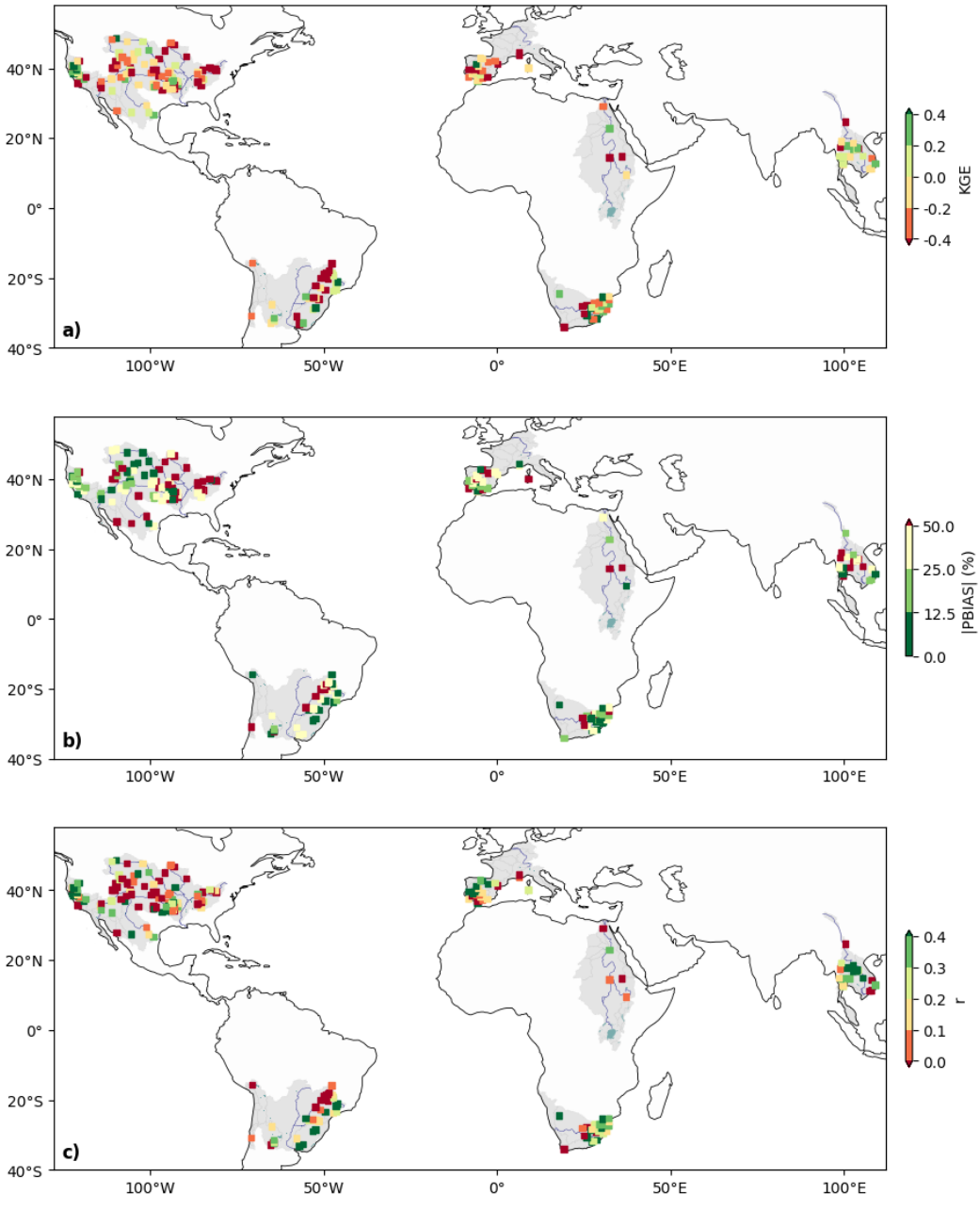

Figure B- 1: Spatial distribution of model performance statistics a) KGE, b) |PBIAS| , and c) Coefficient of Correlation (r) for reservoir storage.

https://doi.org/10.5194/egusphere-2026-881
Preprint. Discussion started: 5 March 2026

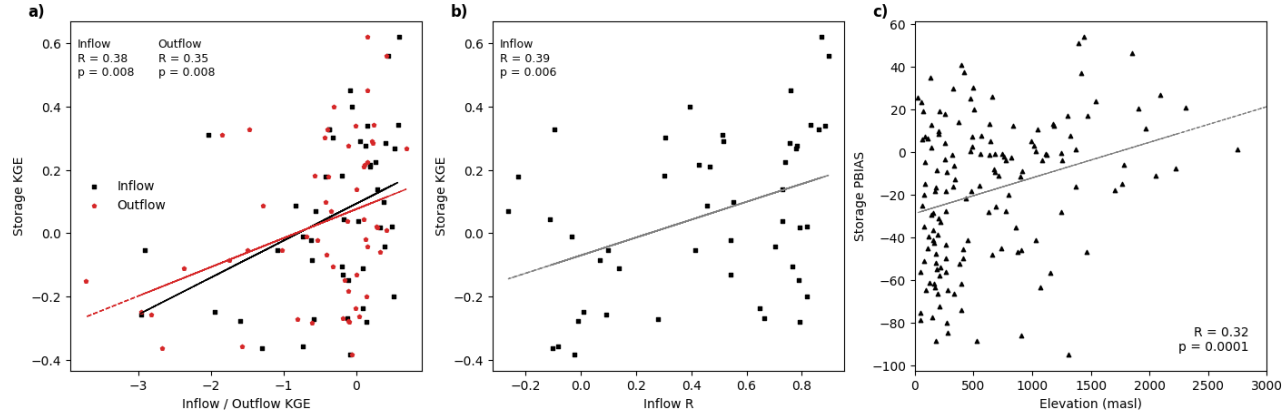

Figure B- 2: Scatter plots showing relationships between reservoir performance metrics, inflow characteristics, and elevation. Panels a) and b) include only reservoirs with monthly storage KGE greater than –0.42, comparing monthly storage KGE with a) monthly inflow

KGE skill score to identify significantly influenced streamflow stations

The change in performance by new implementations was then quantified using the KGE skill score (Towner et al., 2019) :

$$KGE_{SS} = \frac{KGE_{with} - KGE_{without}}{1 - KGE_{without}} \quad \textbf{(B- 1)}$$

Where KGE_{with} and $KGE_{without}$ denote the model performance with and without the new implementations, respectively. The KGE skill score was used mainly as a filtering criterion to distinguish meaningful changes in performance: stations where $|KGE_{SS}|$ were below 0.05 and were considered not to exhibit significant changes and were therefore excluded from further analysis.

https://doi.org/10.5194/egusphere-2026-881
Preprint. Discussion started: 5 March 2026

References

Abbaspour, K. C., Rouholahnejad, E., Vaghefi, S., Srinivasan, R., Yang, H., and Kløve, B.: A continental-scale hydrology and water quality model for Europe: Calibration and uncertainty of a high-resolution large-scale SWAT model, J. Hydrol., 524, 733–752, https://doi.org/10.1016/j.jhydrol.2015.03.027, 2015.

Abdellatif, G., Gaafar, I., Van Der Vat, M., Hellegers, P., El-Naggar, H. E.-D., De Miguel Garcia, A., and Seijger, C.: Impact of irrigation modernization and high Aswan Dam inflow on Nile water system efficiency and water reuse in Egypt, Agric. Water Manag., 316, 109576, https://doi.org/10.1016/j.agwat.2025.109576, 2025.

Abrams, M.: ASTER GLOBAL DEM VERSION 3, AND NEW ASTER WATER BODY DATASET, Int. Arch. Photogramm. Remote Sens. Spat. Inf. Sci., XLI-B4, 107–110, https://doi.org/10.5194/isprs-archives-XLI-B4-107-2016, 2016.

Arnold, J. G., Srinivasan, R., Muttiah, R. S., and Williams, J. R.: LARGE AREA HYDROLOGIC MODELING AND ASSESSMENT PART I: MODEL DEVELOPMENT[1], JAWRA J. Am. Water Resour. Assoc., 34, 73–89, https://doi.org/10.1111/j.1752-1688.1998.tb05961.x, 1998.

Arnold, J. G., Moriasi, D. N., Gassman, P. W., Abbaspour, K. C., White, M. J., R. Srinivasan, C. Santhi, R. D. Harmel, A. Van Griensven, M. W. Van Liew, N. Kannan, and M. K. Jha: SWAT: Model Use, Calibration, and Validation, Trans. ASABE, 55, 1491–1508, https://doi.org/10.13031/2013.42256, 2012.

Arnold, J. G., Bieger, K., White, M., Srinivasan, R., Dunbar, J., and Allen, P.: Use of Decision Tables to Simulate Management in SWAT, Water, 10, 713, https://doi.org/10.3390/W10060713, 2018.

Arnold, J. G., Čerkasova, N., White, M. J., Bailey, R., Thorp, K., Jeong, J., Zhang, X., Ugraskan, T., Griensven, A., Rathjens, H., Raj, C., Cai, X., Geter, W. F., David, O., Carlson, J. R., and Le, K. N.: Soil and Water Assessment Tool Plus (SWAT+), , https://doi.org/10.5281/ZENODO.18727784, 2026.

Ayala, A. I., Hinostroza, J. L., Mercado-Bettín, D., Marcé, R., Gosling, S. N., Pierson, D. C., and Sobek, S.: Integration of the Global Water and Lake Sectors within the ISIMIP framework through scaling of streamflow inputs to lakes, Geosci. Model Dev., 19, 41–56, https://doi.org/10.5194/gmd-19-41-2026, 2026.

Bai, B., Mu, L., Ma, C., Chen, G., and Tan, Y.: Extreme water level changes in global lakes revealed by altimetry satellites since the 2000s, Int. J. Appl. Earth Obs. Geoinformation, 127, 103694, https://doi.org/10.1016/j.jag.2024.103694, 2024.

Beck, H. E., McVicar, T. R., Vergopolan, N., Berg, A., Lutsko, N. J., Dufour, A., Zeng, Z., Jiang, X., Van Dijk, A. I. J. M., and Miralles, D. G.: High-resolution (1 km) Köppen-Geiger maps for 1901–2099 based on constrained CMIP6 projections, Sci. Data, 10, 724, https://doi.org/10.1038/s41597-023-02549-6, 2023.

Bieger, K., Arnold, J. G., Rathjens, H., White, M. J., Bosch, D. D., Allen, P. M., Volk, M., and Srinivasan, R.: Introduction to SWAT+, a completely restructured version of the soil and water assessment tool, JAWRA J. Am. Water Resour. Assoc., 53, 115–130, 2017.

Biemans, H., Haddeland, I., Kabat, P., Ludwig, F., Hutjes, R. W. A., Heinke, J., Von Bloh, W., and Gerten, D.: Impact of reservoirs on river discharge and irrigation water supply during the 20th century, Water Resour. Res., 47, 2009WR008929, https://doi.org/10.1029/2009WR008929, 2011.

Burek, P., Satoh, Y., Kahil, T., Tang, T., Greve, P., Smilovic, M., Guillaumot, L., Zhao, F., and Wada, Y.: Development of the Community Water Model (CWatM v1.04) – a high-resolution hydrological model for global and regional assessment of

https://doi.org/10.5194/egusphere-2026-881
Preprint. Discussion started: 5 March 2026

integrated water resources management, Geosci. Model Dev., 13, 3267–3298, https://doi.org/10.5194/gmd-13-3267-2020, 2020.

Calvin, K., Dasgupta, D., Krinner, G., Mukherji, A., Thorne, P. W., Trisos, C., Romero, J., Aldunce, P., Barrett, K., Blanco, G., Cheung, W. W. L., Connors, S., Denton, F., Diongue-Niang, A., Dodman, D., Garschagen, M., Geden, O., Hayward, B., Jones, C., Jotzo, F., Krug, T., Lasco, R., Lee, Y.-Y., Masson-Delmotte, V., Meinshausen, M., Mintenbeck, K., Mokssit, A., Otto, F. E. L., Pathak, M., Pirani, A., Poloczanska, E., Pörtner, H.-O., Revi, A., Roberts, D. C., Roy, J., Ruane, A. C., Skea, J., Shukla, P. R., Slade, R., Slangen, A., Sokona, Y., Sörensson, A. A., Tignor, M., Van Vuuren, D., Wei, Y.-M., Winkler, H., Zhai, P., Zommers, Z., Hourcade, J.-C., Johnson, F. X., Pachauri, S., Simpson, N. P., Singh, C., Thomas, A., Totin, E., Arias, P., Bustamante, M., Elgizouli, I., Flato, G., Howden, M., Méndez-Vallejo, C., Pereira, J. J., Pichs-Madruga, R., Rose, S. K., Saheb, Y., Sánchez Rodríguez, R., Ürge-Vorsatz, D., Xiao, C., Yassaa, N., Alegría, A., Armour, K., Bednar-Friedl, B., Blok, K., Cissé, G., Dentener, F., Eriksen, S., Fischer, E., Garner, G., Guivarch, C., Haasnoot, M., Hansen, G., Hauser, M., Hawkins, E., Hermans, T., Kopp, R., Leprince-Ringuet, N., Lewis, J., Ley, D., Ludden, C., Niamir, L., Nicholls, Z., Some, S., Szopa, S., Trewin, B., Van Der Wijst, K.-I., Winter, G., Witting, M., Birt, A., Ha, M., et al.: IPCC, 2023: Climate Change 2023: Synthesis Report. Contribution of Working Groups I, II and III to the Sixth Assessment Report of the Intergovernmental Panel on Climate Change [Core Writing Team, H. Lee and J. Romero (eds.)]. IPCC, Geneva, Switzerland., Intergovernmental Panel on Climate Change (IPCC), https://doi.org/10.59327/IPCC/AR6-9789291691647, 2023.

Chawanda, C. J. and Teran, J. P.: jopator/CoSWAT-Framework: CoSWAT-Framework: Integrated reservoirs and lakes., , https://doi.org/10.5281/ZENODO.18746453, 2026.

Chawanda, C. J., Arnold, J., Thiery, W., and Van Griensven, A.: Mass balance calibration and reservoir representations for large-scale hydrological impact studies using SWAT+, Clim. Change, 163, 1307–1327, https://doi.org/10.1007/s10584-020-02924-x, 2020a.

Chawanda, C. J., George, C., Thiery, W., Griensven, A. V., Tech, J., Arnold, J., and Srinivasan, R.: User-friendly workflows for catchment modelling: Towards reproducible SWAT+ model studies, Environ. Model. Softw., 134, 104812, https://doi.org/10.1016/j.envsoft.2020.104812, 2020b.

Chawanda, C. J., Nkwasa, A., Thiery, W., and Van Griensven, A.: Combined impacts of climate and land-use change on future water resources in Africa, Hydrol. Earth Syst. Sci., 28, 117–138, https://doi.org/10.5194/hess-28-117-2024, 2024.

Chawanda, C. J., Van Griensven, A., Nkwasa, A., Teran Orsini, J. P., Jeong, J., Choi, S.-K., Srinivasan, R., and Arnold, J. G.: CoSWAT Model v1: A high-resolution global SWAT+ hydrological model, Hydrol. Earth Syst. Sci., 29, 6901–6916, https://doi.org/10.5194/hess-29-6901-2025, 2025.

Coe, M. T.: Modeling Terrestrial Hydrological Systems at the Continental Scale: Testing the Accuracy of an Atmospheric GCM, J. Clim., 13, 686–704, https://doi.org/10.1175/1520-0442(2000)013%253C0686:MTHSAT%253E2.0.CO;2, 2000.

Dang, T. D., Vu, D. T., Chowdhury, A. F. M. K., and Galelli, S.: A software package for the representation and optimization of water reservoir operations in the VIC hydrologic model, Environ. Model. Softw., 126, 104673, https://doi.org/10.1016/j.envsoft.2020.104673, 2020a.

Dang, T. D., Chowdhury, A. F. M. K., and Galelli, S.: On the representation of water reservoir storage and operations in large-scale hydrological models: implications on model parameterization and climate change impact assessments, Hydrol. Earth Syst. Sci., 24, 397–416, https://doi.org/10.5194/hess-24-397-2020, 2020b.

Döll, P., Kaspar, F., and Lehner, B.: A global hydrological model for deriving water availability indicators: model tuning and validation, J. Hydrol., 270, 105–134, https://doi.org/10.1016/S0022-1694(02)00283-4, 2003.

https://doi.org/10.5194/egusphere-2026-881
Preprint. Discussion started: 5 March 2026

ESA: Land Cover CCI Product User Guide Version 2, 2017.

Fenocchi, A., Rogora, M., Sibilla, S., and Dresti, C.: Relevance of inflows on the thermodynamic structure and on the modeling of a deep subalpine lake (Lake Maggiore, Northern Italy/Southern Switzerland), Limnologica, 63, 42–56, https://doi.org/10.1016/j.limno.2017.01.006, 2017.

Fischer, G., Nachtergaele, F., Prieler, S., van Velthuizen, H. T., Verelst, L., and Wiberg, D.: Harmonized World Soil Database (1.2), 2008.

Gharari, S., Vanderkelen, I., Tefs, A., Mizukami, N., Kluzek, E., Stadnyk, T., Lawrence, D., and Clark, M. P.: A Flexible Framework for Simulating the Water Balance of Lakes and Reservoirs From Local to Global Scales: mizuRoute-Lake, Water Resour. Res., 60, e2022WR032400, https://doi.org/10.1029/2022WR032400, 2024.

Golub, M., Thiery, W., Marcé, R., Pierson, D., Vanderkelen, I., Mercado-Bettin, D., Woolway, R. I., Grant, L., Jennings, E., Kraemer, B. M., Schewe, J., Zhao, F., Frieler, K., Mengel, M., Bogomolov, V. Y., Bouffard, D., Côté, M., Couture, R.-M., Debolskiy, A. V., Droppers, B., Gal, G., Guo, M., Janssen, A. B. G., Kirillin, G., Ladwig, R., Magee, M., Moore, T., Perroud, M., Piccolroaz, S., Raaman Vinnaa, L., Schmid, M., Shatwell, T., Stepanenko, V. M., Tan, Z., Woodward, B., Yao, H., Adrian, R., Allan, M., Anneville, O., Arvola, L., Atkins, K., Boegman, L., Carey, C., Christianson, K., De Eyto, E., DeGasperi, C., Grechushnikova, M., Hejzlar, J., Joehnk, K., Jones, I. D., Laas, A., Mackay, E. B., Mammarella, I., Markensten, H., McBride, C., Özkundakci, D., Potes, M., Rinke, K., Robertson, D., Rusak, J. A., Salgado, R., Van Der Linden, L., Verburg, P., Wain, D., Ward, N. K., Wollrab, S., and Zdorovennova, G.: A framework for ensemble modelling of climate change impacts on lakes worldwide: the ISIMIP Lake Sector, Geosci. Model Dev., 15, 4597–4623, https://doi.org/10.5194/gmd-15-4597-2022, 2022.

Gosling, S. N., Müller Schmied, H., Burek, P., Guillaumot, L., Hanasaki, N., Kou-Giesbrecht, S., Otta, K., Sahu, R.-K., Satoh, Y., and Schewe, J.: ISIMIP3b Simulation Data from the Global Water Sector (1.1), https://doi.org/10.48364/ISIMIP.230418.1, 2024.

Grant, L., Vanderkelen, I., Gudmundsson, L., Tan, Z., Perroud, M., Stepanenko, V. M., Debolskiy, A. V., Droppers, B., Janssen, A. B. G., Woolway, R. I., Choulga, M., Balsamo, G., Kirillin, G., Schewe, J., Zhao, F., Del Valle, I. V., Golub, M., Pierson, D., Marcé, R., Seneviratne, S. I., and Thiery, W.: Attribution of global lake systems change to anthropogenic forcing, Nat. Geosci., 14, 849–854, https://doi.org/10.1038/s41561-021-00833-x, 2021.

Gudmundsson, L., Boulange, J., Do, H. X., Gosling, S. N., Grillakis, M. G., Koutroulis, A. G., Leonard, M., Liu, J., Müller Schmied, H., Papadimitriou, L., Pokhrel, Y., Seneviratne, S. I., Satoh, Y., Thiery, W., Westra, S., Zhang, X., and Zhao, F.: Globally observed trends in mean and extreme river flow attributed to climate change, Science, 371, 1159–1162, https://doi.org/10.1126/science.aba3996, 2021.

Haddeland, I., Skaugen, T., and Lettenmaier, D. P.: Anthropogenic impacts on continental surface water fluxes, Geophys. Res. Lett., 33, 2006GL026047, https://doi.org/10.1029/2006GL026047, 2006.

Haddeland, I., Heinke, J., Biemans, H., Eisner, S., Flörke, M., Hanasaki, N., Konzmann, M., Ludwig, F., Masaki, Y., Schewe, J., Stacke, T., Tessler, Z. D., Wada, Y., and Wisser, D.: Global water resources affected by human interventions and climate change, Proc. Natl. Acad. Sci., 111, 3251–3256, https://doi.org/10.1073/pnas.1222475110, 2014.

Hanasaki, N., Kanae, S., and Oki, T.: A reservoir operation scheme for global river routing models, J. Hydrol., 327, 22–41, https://doi.org/10.1016/j.jhydrol.2005.11.011, 2006.

Hanasaki, N., Yoshikawa, S., Pokhrel, Y., and Kanae, S.: A global hydrological simulation to specify the sources of water used by humans, Hydrol. Earth Syst. Sci., 22, 789–817, https://doi.org/10.5194/hess-22-789-2018, 2018.

https://doi.org/10.5194/egusphere-2026-881
Preprint. Discussion started: 5 March 2026

Hosseini-Moghari, S.-M. and Döll, P.: The value of observed reservoir storage anomalies for improving the simulation of reservoir dynamics in large-scale hydrological models, Hydrol. Earth Syst. Sci., 29, 4073–4092, https://doi.org/10.5194/hess-29-4073-2025, 2025.

Janssen, A. B., Janse, J. H., Beusen, A. H., Chang, M., Harrison, J. A., Huttunen, I., Kong, X., Rost, J., Teurlincx, S., Troost, T. A., Van Wijk, D., and Mooij, W. M.: How to model algal blooms in any lake on earth, Curr. Opin. Environ. Sustain., 36, 1–10, https://doi.org/10.1016/j.cosust.2018.09.001, 2019.

Khazaei, B., Read, L. K., Casali, M., Sampson, K. M., and Yates, D. N.: GLOBathy, the global lakes bathymetry dataset, Sci. Data, 9, 36, https://doi.org/10.1038/s41597-022-01132-9, 2022.

Knoben, W. J. M., Freer, J. E., and Woods, R. A.: Technical note: Inherent benchmark or not? Comparing Nash–Sutcliffe and Kling–Gupta efficiency scores, Hydrol. Earth Syst. Sci., 23, 4323–4331, https://doi.org/10.5194/hess-23-4323-2019, 2019.

Kumar, A., Gosling, S. N., Johnson, M. F., Jones, M. D., Zaherpour, J., Kumar, R., Leng, G., Schmied, H. M., Kupzig, J., Breuer, L., Hanasaki, N., Tang, Q., Ostberg, S., Stacke, T., Pokhrel, Y., Wada, Y., and Masaki, Y.: Multi-model evaluation of catchment- and global-scale hydrological model simulations of drought characteristics across eight large river catchments, Adv. Water Resour., 165, 104212, https://doi.org/10.1016/j.advwatres.2022.104212, 2022.

La Fuente, S., Jennings, E., Lenters, J. D., Verburg, P., Kirillin, G., Shatwell, T., Couture, R.-M., Côté, M., Vinnå, C. L. R., and Woolway, R. I.: Increasing warm-season evaporation rates across European lakes under climate change, Clim. Change, 177, 173, https://doi.org/10.1007/s10584-024-03830-2, 2024.

Lange, S., Mengel, M., Treu, S., and Büchner, M.: ISIMIP3a atmospheric climate input data (1.2), https://doi.org/10.48364/ISIMIP.982724.2, 2022.

Lehner, B. and Grill, G.: Global river hydrography and network routing: baseline data and new approaches to study the world's large river systems, Hydrol. Process., 27, 2171–2186, https://doi.org/10.1002/hyp.9740, 2013.

Lehner, B., Liermann, C. R., Revenga, C., Vörösmarty, C., Fekete, B., Crouzet, P., Döll, P., Endejan, M., Frenken, K., Magome, J., Nilsson, C., Robertson, J. C., Rödel, R., Sindorf, N., and Wisser, D.: High-resolution mapping of the world's reservoirs and dams for sustainable river-flow management, Front. Ecol. Environ., 9, 494–502, https://doi.org/10.1890/100125, 2011.

Li, Y.: Global Reservoir Storage (GRS) dataset, https://doi.org/10.5281/ZENODO.7855477, 2023.

Meigh, J. R., McKenzie, A. A., and Sene, K. J.: A Grid-Based Approach to Water Scarcity Estimates for Eastern and Southern Africa, Water Resour. Manag., 13, 85–115, https://doi.org/10.1023/A:1008025703712, 1999.

Messager, M. L., Lehner, B., Grill, G., Nedeva, I., and Schmitt, O.: Estimating the volume and age of water stored in global lakes using a geo-statistical approach, Nat. Commun., 7, 13603, https://doi.org/10.1038/ncomms13603, 2016.

Moriasi, D. N., J. G. Arnold, M. W. Van Liew, R. L. Bingner, R. D. Harmel, and T. L. Veith: Model Evaluation Guidelines for Systematic Quantification of Accuracy in Watershed Simulations, Trans. ASABE, 50, 885–900, https://doi.org/10.13031/2013.23153, 2007.

Neitsch, S. L., Arnold, J. G., Kiniry, J. R., and Williams, J. R.: Soil and water asessment tool theoritical documentation: version 2009. Texas Water Resources Institute technical report No. 406., 2011.

https://doi.org/10.5194/egusphere-2026-881
Preprint. Discussion started: 5 March 2026

Nkwasa, A., Chawanda, C. J., Jägermeyr, J., and Van Griensven, A.: Improved representation of agricultural land use and crop management for large-scale hydrological impact simulation in Africa using SWAT+, Hydrol. Earth Syst. Sci., 26, 71–89, https://doi.org/10.5194/hess-26-71-2022, 2022a.

Nkwasa, A., Chawanda, C. J., and Van Griensven, A.: Regionalization of the SWAT+ model for projecting climate change impacts on sediment yield: An application in the Nile basin, J. Hydrol. Reg. Stud., 42, 101152, https://doi.org/10.1016/j.ejrh.2022.101152, 2022b.

Nkwasa, A., Chawanda, C. J., Theresa Nakkazi, M., Tang, T., Eisenreich, S. J., Warner, S., and Van Griensven, A.: One third of African rivers fail to meet the 'good ambient water quality' nutrient targets, Ecol. Indic., 166, 112544, https://doi.org/10.1016/j.ecolind.2024.112544, 2024.

Nkwasa, A., James Chawanda, C., Theresa Nakkazi, M., and Van Griensven, A.: CoSWAT-WQ v1.0: a high-resolution community global SWAT+ water quality model, https://doi.org/10.5194/egusphere-2025-703, 24 February 2025.

Perera, D., Williams, S., and Smakhtin, V.: Present and Future Losses of Storage in Large Reservoirs Due to Sedimentation: A Country-Wise Global Assessment, Sustainability, 15, 219, https://doi.org/10.3390/su15010219, 2022.

Pillco Zolá, R., Bengtsson, L., Berndtsson, R., Martí-Cardona, B., Satgé, F., Timouk, F., Bonnet, M.-P., Mollericon, L., Gamarra, C., and Pasapera, J.: Modelling Lake Titicaca's daily and monthly evaporation, Hydrol. Earth Syst. Sci., 23, 657–668, https://doi.org/10.5194/hess-23-657-2019, 2019.

Pokhrel, Y. N., Hanasaki, N., Wada, Y., and Kim, H.: Recent progresses in incorporating human land–water management into global land surface models toward their integration into Earth system models, WIREs Water, 3, 548–574, https://doi.org/10.1002/wat2.1150, 2016.

Porkka, M., Virkki, V., Wang-Erlandsson, L., Gerten, D., Gleeson, T., Mohan, C., Fetzer, I., Jaramillo, F., Staal, A., te Wierik, S., Tobian, A., van der Ent, R., Döll, P., Flörke, M., Gosling, S. N., Hanasaki, N., Satoh, Y., Müller Schmied, H., Wanders, N., Famiglietti, J. S., Rockström, J., and Kummu, M.: Notable shifts beyond pre-industrial streamflow and soil moisture conditions transgress the planetary boundary for freshwater change, Nat. Water, 2, 262–273, https://doi.org/10.1038/s44221-024-00208-7, 2024.

Shin, S., Pokhrel, Y., and Miguez-Macho, G.: High-Resolution Modeling of Reservoir Release and Storage Dynamics at the Continental Scale, Water Resour. Res., 55, 787–810, https://doi.org/10.1029/2018WR023025, 2019.

Shin, S., Pokhrel, Y., Yamazaki, D., Huang, X., Torbick, N., Qi, J., Pattanakiat, S., Ngo-Duc, T., and Nguyen, T. D.: High Resolution Modeling of River-Floodplain-Reservoir Inundation Dynamics in the Mekong River Basin, Water Resour. Res., 56, e2019WR026449, https://doi.org/10.1029/2019WR026449, 2020.

Shrestha, P. K., Samaniego, L., Rakovec, O., Kumar, R., Mi, C., Rinke, K., and Thober, S.: Toward Improved Simulations of Disruptive Reservoirs in Global Hydrological Modeling, Water Resour. Res., 60, e2023WR035433, https://doi.org/10.1029/2023WR035433, 2024.

Siebert, S., Henrich, V., Frenken, K., and Burke, J.: Global Map of Irrigation Areas version 5, 2013.

Steyaert, J. C., Condon, L. E., W.D. Turner, S., and Voisin, N.: ResOpsUS, a dataset of historical reservoir operations in the contiguous United States, Sci. Data, 9, 34, https://doi.org/10.1038/s41597-022-01134-7, 2022.

https://doi.org/10.5194/egusphere-2026-881
Preprint. Discussion started: 5 March 2026

Tang, L., Liu, G., Sun, X., and Liu, P.: Optimizing storage-based reservoir operation schemes for enhanced large-scale hydrological modeling: A comprehensive sensitivity analysis, J. Hydrol., 657, 133173, https://doi.org/10.1016/j.jhydrol.2025.133173, 2025.

Tarboton, G. D., K. A. T. Schreuders, D. W. Watson, and M. E. Baker: Generalized terrain-based flow analysis of digital elevation models, 18th World IMACS Congress and MODSIM09 International Congress on Modelling and Simulation, 2009.

Telteu, C.-E., Müller Schmied, H., Thiery, W., Leng, G., Burek, P., Liu, X., Boulange, J. E. S., Andersen, L. S., Grillakis, M., Gosling, S. N., Satoh, Y., Rakovec, O., Stacke, T., Chang, J., Wanders, N., Shah, H. L., Trautmann, T., Mao, G., Hanasaki, N., Koutroulis, A., Pokhrel, Y., Samaniego, L., Wada, Y., Mishra, V., Liu, J., Döll, P., Zhao, F., Gädeke, A., Rabin, S. S., and Herz, F.: Understanding each other's models: an introduction and a standard representation of 16 global water models to support intercomparison, improvement, and communication, Geosci. Model Dev., 14, 3843–3878, https://doi.org/10.5194/gmd-14-3843-2021, 2021.

Teran, J. P.: Integrating reservoirs and Lakes in the CoSWAT model., https://doi.org/10.5281/ZENODO.18733431, 2026a.

Teran, J. P.: jopator/teran_2026_coswat_reservoirs: teran_2026, , https://doi.org/10.5281/ZENODO.18746130, 2026b.

Terink, W., Lutz, A. F., Simons, G. W. H., Immerzeel, W. W., and Droogers, P.: SPHY v2.0: Spatial Processes in HYdrology, Geosci. Model Dev., 8, 2009–2034, https://doi.org/10.5194/gmd-8-2009-2015, 2015.

Thompson, J. R., Gosling, S. N., Zaherpour, J., and Laizé, C. L. R.: Increasing Risk of Ecological Change to Major Rivers of the World With Global Warming, Earths Future, 9, e2021EF002048, https://doi.org/10.1029/2021EF002048, 2021.

Towner, J., Cloke, H. L., Zsoter, E., Flamig, Z., Hoch, J. M., Bazo, J., Coughlan De Perez, E., and Stephens, E. M.: Assessing the performance of global hydrological models for capturing peak river flows in the Amazon basin, Hydrol. Earth Syst. Sci., 23, 3057–3080, https://doi.org/10.5194/hess-23-3057-2019, 2019.

Vanderkelen, I., Van Lipzig, N. P. M., and Thiery, W.: Modelling the water balance of Lake Victoria (East Africa) – Part 1: Observational analysis, Hydrol. Earth Syst. Sci., 22, 5509–5525, https://doi.org/10.5194/hess-22-5509-2018, 2018.

Vanderkelen, I., Gharari, S., Mizukami, N., Clark, M. P., Lawrence, D. M., Swenson, S., Pokhrel, Y., Hanasaki, N., Van Griensven, A., and Thiery, W.: Evaluating a reservoir parametrization in the vector-based global routing model mizuRoute (v2.0.1) for Earth system model coupling, Geosci. Model Dev., 15, 4163–4192, https://doi.org/10.5194/gmd-15-4163-2022, 2022.

Wisser, D., Frolking, S., Hagen, S., and Bierkens, M. F. P.: Beyond peak reservoir storage? A global estimate of declining water storage capacity in large reservoirs: Beyond Peak Reservoir Storage?, Water Resour. Res., 49, 5732–5739, https://doi.org/10.1002/wrcr.20452, 2013.

Woolway, R. I. and Merchant, C. J.: Worldwide alteration of lake mixing regimes in response to climate change, Nat. Geosci., 12, 271–276, https://doi.org/10.1038/s41561-019-0322-x, 2019.

Wu, J., Yen, H., Arnold, J. G., Yang, Y. C. E., Cai, X., White, M. J., Santhi, C., Miao, C., and Srinivasan, R.: Development of reservoir operation functions in SWAT+ for national environmental assessments, J. Hydrol., 583, 124556, https://doi.org/10.1016/j.jhydrol.2020.124556, 2020.

Yassin, F.: Reservoir inflow, storage and realease, https://doi.org/10.5281/ZENODO.1492043, 2018.

https://doi.org/10.5194/egusphere-2026-881
Preprint. Discussion started: 5 March 2026

Yassin, F., Razavi, S., Elshamy, M., Davison, B., Sapriza-Azuri, G., and Wheater, H.: Representation and improved parameterization of reservoir operation in hydrological and land-surface models, Hydrol. Earth Syst. Sci., 23, 3735–3764, https://doi.org/10.5194/hess-23-3735-2019, 2019.

Zajac, Z., Revilla-Romero, B., Salamon, P., Burek, P., Hirpa, F. A., and Beck, H.: The impact of lake and reservoir parameterization on global streamflow simulation, J. Hydrol., 548, 552–568, https://doi.org/10.1016/j.jhydrol.2017.03.022, 2017.

Zhao, G. and Gao, H.: Estimating reservoir evaporation losses for the United States: Fusing remote sensing and modeling approaches, Remote Sens. Environ., 226, 109–124, https://doi.org/10.1016/j.rse.2019.03.015, 2019.